[American Journal of Science, Vol. 315, January, 2015, P. 46–76, DOI 10.2475/01.2015.02]

EROSION RATES IN AND AROUND SHENANDOAH NATIONAL PARK, VIRGINIA, DETERMINED USING ANALYSIS OF COSMOGENIC ^{10}Be

JANE DUXBURY*, PAUL R. BIERMAN*,†, ERIC W. PORTENGA*,§, MILAN J. PAVICH**, SCOTT SOUTHWORTH**, and STEWART P.H.T. FREEMAN***

ABSTRACT. **We use cosmogenic ^{10}Be analysis of fluvial sediments and bedrock to estimate erosion rates (10^4-10^5 year timescale) and to infer the distribution of post-orogenic geomorphic processes in the Blue Ridge Province in and around Shenandoah National Park, Virginia. Our sampling plan was designed to investigate relationships between erosion rate and lithology, mean basin slope, basin area, and sediment grain size. Fifty-nine samples were collected from a variety of basin sizes (<1-3305 km^2) and average basin slopes (6-24°) in each of four different lithologies that crop out in the park: granite, metabasalt, quartzite, and siliciclastic rocks. The samples include bedrock (n = 5), fluvial sediment from single-lithology basins (n = 43), and fluvial sediment from multilithology basins (n = 11): two multilithology samples are from rivers with tributary streams draining the eastern and western slopes of the park, respectively (Rappahannock and Shenandoah Rivers), and two samples are temporal replicates. In one sample of each lithology, we measured ^{10}Be in four different grain sizes from fine sand to gravel.**

Inferred erosion rates for the medium sand fraction of all fluvial samples from all lithologies range from 3.0 to 21 m/My. The area-weighted mean erosion rate for single-lithology basins in the Park is 12.2 m/My. Single-lithology erosion rate ranges for fluvial samples are: granite, 7.0 to 20 m/My; metabasalt, 3.8 to 21 m/My; quartzite, 3.8 to 15 m/My; and siliciclastic rocks, 5.2 to 15 m/My. Multilithology basins erode at rates between 3.0-16 m/My. The Shenandoah River basin (3305 km^2) is eroding at 6.6 m/My. Bedrock erosion rates range from 1.8 to 11 m/My across all lithologies, with a mean of 6.5 ± 4.3 m/My. Grain-size specific ^{10}Be analysis of four samples showed no consistent trend of concentration with grain size.

Cosmogenic analysis of bedrock and sediment from the Shenandoah National Park area allows us to speculate about why some parts of the Appalachian Mountains erode more slowly and some more rapidly. Overall, it appears that steep drainage basins erode more rapidly than gently sloped basins. Climate and lithology may also influence basin-scale rates of erosion as suggested by the difference in average erosion rates east and west of the divide and the difference between the erosion rates of quartzite- and granite-dominated basins. Data are conflicting in regards to the evolution of relief over time. Analyses made of exposed bedrock along ridgelines suggest that such rock is eroding either more slowly than adjacent drainage basins (Susquehanna River, Shenandoah National Park region) or at similar rates (Great Smoky Mountains) providing a mechanism for growing relief at the scale of individual ridgelines. However, considering relief on a landscape or physiographic province scale, by comparing erosion rates of the highlands versus the lowlands, suggests that relief of the range as a whole is either steady or very slowly decreasing over multi-millennial timescales. The presence of significant erosion rate/slope relationships negates a broad Hackian view of the landscape because there is not uniform erosion across this landscape. The aspect-erosion rate and slope-erosion rate relationships present in the Shenandoah area suggest that the landscape is not fully adjusted to rock strength.

* Geology Department, University of Vermont, Burlington, Vermont 05405
** U.S. Geological Survey, Reston, Virginia 20192
*** SUERC, Accelerator Mass Spectrometry Laboratory, East Kilbride, Scotland
§ Present address: University of Glasgow, School of Geographical and Earth Science, Lilybank Gardens, Glasgow G12 8QQ, United Kingdom, and Macquarie University, Department of Environment and Geography, North Ryde NSW 2109, Australia
† Corresponding author: pbierman@uvm.edu

Key words: Erosion, cosmogenic, Appalachian, geomorphology, isotope geology

INTRODUCTION

Understanding the dynamic nature of the Earth's surface and the rate at which the landscape has changed over time are fundamental to geomorphology. Geomorphologists have long sought to understand the relationships between erosion (both physical and chemical, for example, Riebe and others, 2001b; Riebe and others, 2003), climate (Harris and Mix, 2002), topography, and lithology (Hack, 1960). Over the last decade, the development and widespread application of cosmogenic and thermochronologic techniques capable of quantitatively estimating rates of erosion has revolutionized our understanding of Earth's dynamic surface (Nishiizumi and others, 1986; Bierman and Nichols, 2004; Reiners and Brandon, 2006; Bishop, 2007; Portenga and Bierman, 2011). To this end, we utilize cosmogenic ^{10}Be in order to explore the relationship between erosion rate, lithology, slope, aspect and basin area, as well as the relationship between ^{10}Be concentration and grain size, in order to learn more about landscape evolution and test Hack's (1960) model of *dynamic equilibrium* and steady state behavior in the Blue Ridge Province in and around Shenandoah National Park, Virginia.

The Appalachian Mountains have been the subject of intense study for more than a century (Davis, 1899; Hack, 1960; Barron, 1989; Pavich, 1990; Pazzaglia and Gardner, 1994; Granger and others, 1997; Eaton and others, 2003a; Ward and others, 2005; Hancock and Kirwan, 2007). These mountains are of particular interest because they are an easily accessible natural laboratory in which to understand better the geomorphic processes that occur on passive margin mountain ranges after orogenesis (Pazzaglia and Brandon, 1996). Of particular interest in the Appalachian Mountains is the apparent paradox of mountainous topography existing hundreds of millions of years after the cessation of convergent orogenic activity (Rodgers, 1970).

In the broader context of aging orogens, and as part of a series of cosmogenic studies of the Appalachian Mountains (Matmon and others, 2003a; Matmon and others, 2003b; Reuter, ms, 2005; Sullivan and others, 2006; Hancock and Kirwan, 2007; Whitten, ms, 2009; Trodick and others, 2010; Miller and others, 2013; Portenga and others, 2013), this research investigates millennial-time-scale erosion rates in the Shenandoah National Park region, Virginia, using 71 measurements of *in situ* produced cosmogenic ^{10}Be derived from fluvial sediments and bedrock. The sizes of sampled drainage basins are constrained by the lithology of the area and range from <1 to 3305 km^2. Our findings can be compared with the several hundred cosmogenic nuclide analyses made along the length of the Appalachian Mountains.

BACKGROUND

Appalachian Mountain Physiography and History

The Appalachian Mountains extend from Newfoundland, Canada in the northeast, southwest to Alabama (Rodgers, 1970). In the Mid-Atlantic region, the mountain belt and adjacent area is divided into five physiographic provinces. From west to east, these are the Appalachian Plateau, the Valley and Ridge, the Blue Ridge, the Piedmont, and the Coastal Plain (Gathright, 1976).

The Appalachian Plateau lies to the northwest of the Valley and Ridge Province (fig. 1) and it is separated from the Valley and Ridge by the Allegheny structural front, an escarpment at the transition from the tight folds of the Valley and Ridge to the low-amplitude folds and flat-lying, gently folded strata of the Plateau (sandstones, conglomerates, shales, and coal). The Valley and Ridge consists of linear, parallel ridges of siliciclastic rocks and valleys largely underlain by carbonate rocks. This topography is thought to be the result of differential weathering and erosion of the heavily faulted and folded rocks (Rodgers, 1970).

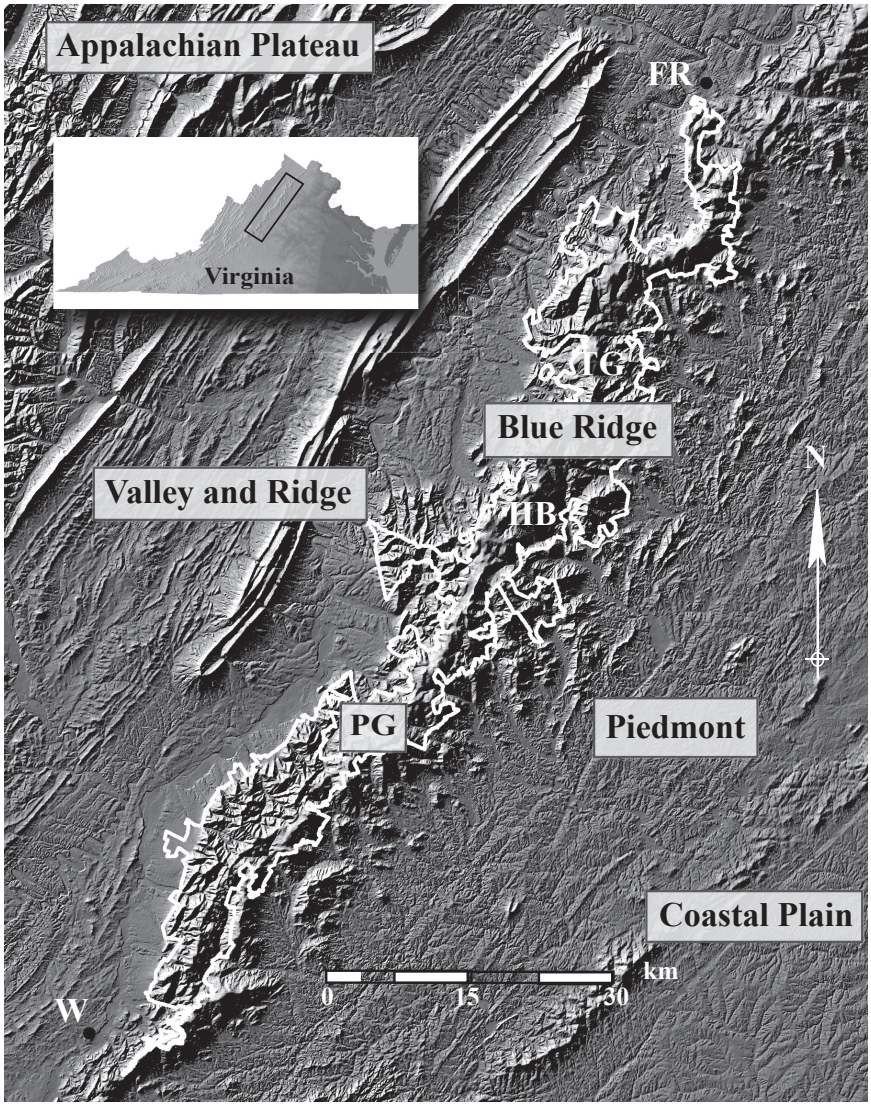

Fig. 1. Shaded digital elevation model of north-central Virginia showing the Shenandoah Region and adjacent physiographic provinces. White line is Shenandoah National Park boundary. Inset shows the location of the park in Virginia. FR = Front Royal, W = Waynesboro, HB = Hawksbill, TG = Thornton Gap, PG = Powell Gap. (Data source: US Geological Survey).

The Blue Ridge Province is a highland that abruptly rises hundreds of meters above sea level and is situated between the Piedmont to its east and the Valley and Ridge Province to its west (fig. 1). It is an allochthonous anticlinorium with a core of Mesoproterozoic crystalline rocks flanked by metamorphosed sedimentary and volcanic rocks (Tollo and others, 2004).

The Piedmont Province is a low-relief area to the east of the Blue Ridge Province (fig. 1). It is characterized by gently rolling topography, few outcrops, and bedrock that is deeply weathered to saprolite (Pavich, 1985). The Piedmont is underlain by a variety of Paleozoic to Mesozoic igneous, metamorphic, and sedimentary rocks. Low-relief

interior basins of the Piedmont contain diabase dikes, basalt flows, and isolated sedimentary rocks, which are located in half-graben basins formed during the early stages of rifting associated with the opening of the Atlantic Ocean (Hack, 1982; Pavich, 1985).

The Coastal Plain is east of the Piedmont Province and Fall Zone (falls and rapids of streams flowing across the rocks of the Piedmont onto the unconsolidated sediments of the Coastal Plain), and extends to the Atlantic Ocean (fig. 1). The Coastal Plain is characterized by Cretaceous and Tertiary sediments that overly the igneous and metamorphic bedrock of the Piedmont (Stanford and others, 2002).

Evolution of the Appalachian Mountain Belt.—Landscape evolution in the Appalachians has been much studied over the last century spawning concepts such as William Morris Davis' *Geographic Cycle* (1899) and J.T. Hack's model of *Dynamic Equilibrium* (1960). The *Geographic Cycle* (1899) posits how mean relief and mean elevation change directionally as a landscape erodes, focusing on transport-limited processes and the flattening of hillslopes over time. Conversely, Hack's (1960) model of *Dynamic Equilibrium* asserts that in a landscape there is a constant adjustment between principal resisting and driving forces, relating to rock type, tectonics, and climate. Erosion rates in such a Hackian landscape will be invariant; slope will be related to rock strength.

Evolution of the post-orogenic Appalachian Mountains remains a research focus primarily because of the apparent paradox of continued significant relief in the range despite the cessation of primary orogenic events ~300 m.y.a. Extensional and rifting processes and subsequent flexural deformation of the Atlantic margin provide one mechanism for rejuvenated uplift in the Appalachian Mountains. Pazzaglia and Gardner (1994, 2000) suggest that this mechanism accounts for the existence of 7 km of detritus in offshore Atlantic basins. Another explanation for post-orogenic Appalachian tectonic history and evolution includes pulses of sediment delivered to offshore basins via cycles of tectonic uplift (Hack, 1982) and rapid sediment accumulation (Poag and Sevon, 1989; Pazzaglia, 1993; Pazzaglia and Brandon, 1996).

Cenozoic drainage capture and erosion rate variation.—A model of drainage capture, for the Appalachian Mountains progressive piracy, was proposed initially by Thompson (1939) and has been further expanded by Harbor and others (1998, 2005), Pazzaglia and Gardner (1994, 2000), Naeser and others (2001), and Pazzaglia and others (2006). Thompson (1939) proposed that the original drainage divide was along the Blue Ridge and that due to steeper gradients of slopes, the headward-eroding Atlantic streams captured drainage area from the Gulf of Mexico-bound streams pushing the drainage divide through the Blue Ridge and Valley and Ridge and into the Appalachian Plateau. Pazzaglia and Gardner (1994, 2000) suggest that epierogenic uplift, changes in climate, and/or rapid changes in the size of the Atlantic slope drainage basin may be responsible for the removal of regolith during the middle Miocene and thus drainage divide migration. This drainage capture proceeded from north to south. First the Susquehanna, and then the ancestral Potomac River drainage breached the Blue Ridge and captured the westward flowing drainage (Thompson, 1939; Naeser and others, 2006a).

The re-orientation of Appalachian drainages (Potomac and Susquehanna Rivers) to the east may have been accompanied by and linked to increases of relief and topography, which can be attributed to several factors: asthenosphere flow and magmatism events in the Cretaceous, subsequent post-rift thermal relaxation and asthenospheric flow, and development of dynamically supported topography in the Miocene (Pazzaglia and Brandon, 1996).

On the basis of the offshore sediment record and interpretive models, Pazzaglia and Gardner (1994) and Pazzaglia and Brandon (1996) suggest that after the Alleghenian orogeny, Appalachian erosion rates have varied between ~12 to 44 m/My over

the last ~200 my. They posit that flexural isostatic deformation, a continual uplift process with variable rates modulated by eustatic sea-level variations, drove Cenozoic erosional sediment delivery to offshore basins (Pazzaglia and others, 2006). In the central Appalachians, U-Th/He thermochronologic data and existing apatite fission track (AFT) thermochronology reveal a shift in the drainage divide linked to the accumulation of Miocene sediments on the Coastal Plain. U-Th/He and AFT closure ages are practically indistinguishable over the last ~200 My (Roden, 1991; Blackmer and others, 1994; Boettcher and Milliken, 1994; Reed and others, 2005), suggesting moderate amounts of unroofing (Pazzaglia and others, 2006) which can be interpreted as long term, average erosion rates of 10 to 30 m/My. In the Blue Ridge and Piedmont Provinces, the story is different. There, the U-Th/He ages are younger than the AFT ages in these areas, indicating increased and continuous unroofing during Alleghenian orogenesis and Mesozoic rifting. Long-term average continental denudation rates based on offshore sediment accumulation are likely between ~10 to 20 m/My (Pazzaglia and others, 2006), which is in good agreement with AFT data from the Blue Ridge (Naeser and others, 2004). Together these datasets indicate that the Appalachian Mountain landscape has been eroding on average at ~20 m/My over at least since the Miocene and perhaps much longer, a value consistent with the compilation of Matmon and others (2003a).

Geology and Physiography of the Shenandoah National Park Region

Shenandoah National Park region physiography.—Shenandoah National Park (fig. 1) is situated along the Blue Ridge, a highland area between the towns of Front Royal to the north and Rockfish Gap to the south, near Waynesboro, Virginia. The highlands contain mostly forested uplands; adjacent lowlands are privately held and largely cleared for agriculture. The highest elevation along the ridge within the park is Hawksbill, elevation 1235 m, rising above the low-lying Piedmont Province to the east and the Shenandoah Valley to the west. The Potomac River crosses the Blue Ridge to the north at Harpers Ferry, West Virginia, and the James and Roanoke Rivers cross the Blue Ridge to the south. There are also two major wind gaps, Thornton and Powell, which are thought to mark the path of ancient stream courses (Kiver and others, 1999). Slopes within and near the park are heavily vegetated and often covered by regolith and soil. Ridgelines expose bare rock.

Shenandoah National Park region geology.—The geology of the Shenandoah National Park region, and the rocks we have sampled both from outcrops and in river sediments, have been well studied by King (1950), Reed (1955), Gathright (1976), and Southworth and others (2009). This part of the Blue Ridge Province (figs. 1 and 2) consists of Mesoproterozoic to early Cambrian rocks that record the earliest history of eastern North America. Mesoproterozoic granitic gneisses were emplaced, metamorphosed and deformed ~1 billion years ago during the Grenvillian orogeny (Tollo and others, 2006). Neoproterozoic granites were emplaced, and sediments were deposited prior to the extrusion of flood basalts from 575 to 560 Ma associated with extensional tectonics and continental breakup (Badger and Sinha, 1988; Bailey and others, 2006). As the Laurentian Sea opened, coastal plain deposits covered the subsiding landmass. The rocks were buried, metamorphosed, folded, faulted, and tectonically transported westward to their current geographic position in the late Paleozoic Alleghenian orogeny, forming the Blue Ridge-South Mountain anticlinorium (Southworth and others, 2006). The western limb of this anticlinorium is composed of the lithologies we sampled both in outcrop and as a source of river sediment; granite, metabasalt, quartzite, and siliciclastic rocks (metasiltstone, sandstone, and phyllite).

Following the Alleghenian orogeny, erosional events during the Late Permian and Early Triassic periods transported sediment west to the Appalachian foreland basin. The extensional separation of North America and Africa, beginning at ~200 Ma,

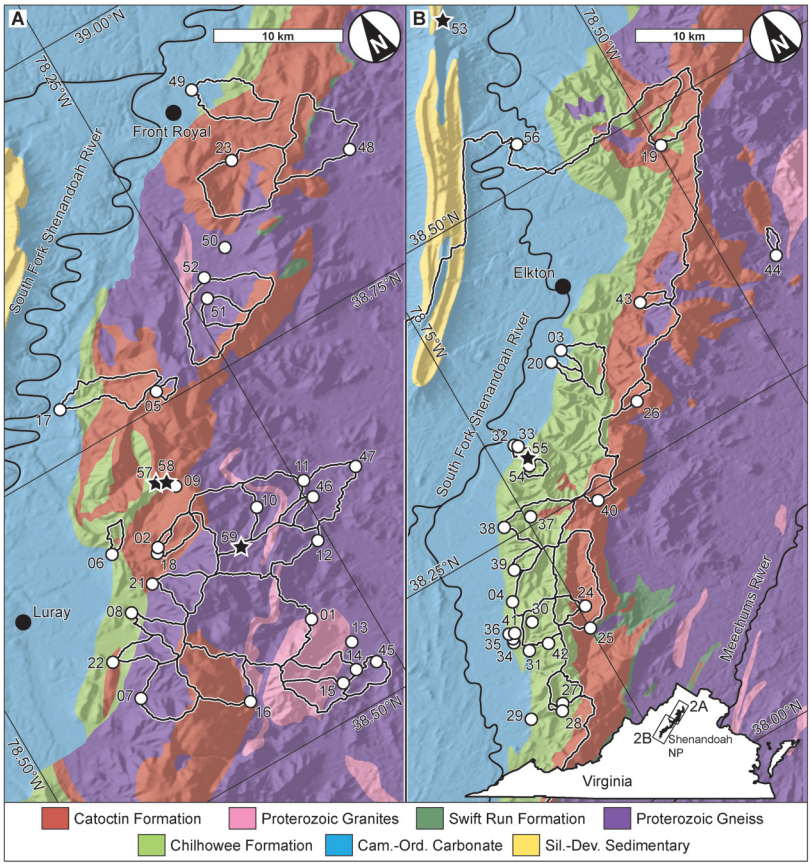

Fig. 2. Sample location map. Inset shows location of close-up maps A and B. Proterozoic gneisses and granitic gneisses make up the bedrock east of the main Blue Ridge crest. The Catoctin Formation comprises the metabasalt designation in this study that is interleaved with phyllites and sandstones of the Swift Run Formation. For the purposes of this study, quartzite combines the Chilhowee, Weverton, Antietam, and Harpers Formations. Siliciclastic designations in this study are found to the west of the Blue Ridge crest. The Silurian-Devonian sediments west of Shenandoah National Park cap Massanutten Ridge. (A) Shaded digital elevation model* of north-central Virginia showing the northern section of the Shenandoah Region with geologic units**. (B) Shaded digital elevation model* of north-central Virginia showing the southern section of the Shenandoah Region with geologic units** (*USGS digital data, http://pubs.usgs.gov/of/2003/0f03-410/, ** Southworth and others, 2009). Sample sites shown with open circles. Towns shown with closed circles. Stars indicate bedrock samples and sampled drainage basins are outlined.

resulted in the opening of the Atlantic Ocean in the early Jurassic and led to the development of the Atlantic passive margin. This rifting likely caused renewed uplift on the rift shoulders and increased relief (Pazzaglia and Brandon, 1996).

Stratigraphy.—There are four principal rock types within and adjacent to the Shenandoah National Park (fig. 2): (1) Mesoproterozoic granitic gneisses underlie the highlands along the Blue Ridge and the lowlands to the east. There are at least 30 different sub-varieties of granitic gneisses that have been mapped (Southworth and others, 2009). (2) Neoproterozoic metabasalt and metasedimentary rocks also underlie the highlands along the Blue Ridge and the lowlands to the east. Metabasalt (with vein quartz) is the dominant rock in the Catoctin Formation (Badger and Sinha, 1988), and the underlying Swift Run Formation consists of local accumulations of sandstone and phyllite. (3) Cambrian quartzite and metasiltstone are restricted to the

boundary of the Blue Ridge and the Valley and Ridge and they underlie distinctive ridges and swales that have lower altitude and relief than the adjacent highlands. The quartzite and metasiltstone constitutes the Chilhowee Group, comprised of the Weverton, Harpers, and Antietam Formations. (4) Cambrian and Ordovician carbonate rocks are restricted to the Valley and Ridge province west of the quartzite ridges. The carbonate rocks that overly the Antietam Formation in the Valley and Ridge are the Tomstown, Waynesboro, Elbrook, and Conococheaque formations.

Geomorphic history of the Shenandoah area.—The landforms within and surrounding the area provide insight into the erosional and geomorphic history of the Shenandoah region. The alluvial fans on the west side of Shenandoah National Park are long-term but undated accumulations of coarse, clastic debris transported by water. The 100 m thickness of these deposits is in part a function of the setting, which is a trap for sediment (Hack, 1965; Kochel and Johnson, 1984; Whittecar, 1992). The coarse fan material has only locally been eroded by modern drainage systems, whereas the carbonate substrate has been lowered by chemical weathering over an extended period. Manganese deposits in the underlying clay residuum, as well as lignitic material, interpreted as Tertiary (Stose and others, 1919) and (or) Late Cretaceous (Pierce, 1965) in age, suggest the chemical lowering of the valley substrate has been active for at least 65 My.

To the east of the park, broad alluvial plains with strath terraces (Morgan and others, 2004) are incised into granitic gneisses, but extensive alluvial or fan deposits are not preserved. The tributaries that drain these plains head in the highlands where basins and hollows are underlain by large boulder deposits related to ancient debris flows and now-inactive periglacial processes (Morgan and others, 2004). Modern intense and long-duration rainfall events have resulted in debris flows east of the park that flushed the coarse debris out of the hollows and deposited them on adjacent lowland valley floors (Morgan and others, 1999; Eaton and others, 2003a; Eaton and others, 2003b). The highlands are underlain in places by a thick mantle of stratified slope deposits (slope wash processes) probably relict from an earlier periglacial climate; these deposits are not a result of modern storm-driven erosion (Litwin and others, 2001; Smoot, 2004). Scree slopes, block fields, and colluvium occur at the high elevations (Gathright, 1976) and locally overlie the older stratified slope deposits (Smoot, 2004).

There is evidence of past, periglacial climates in the high elevations of the Blue Ridge region characterized by mass wasting and freeze-thaw processes (Washburn, 1973; Washburn, 1980). Mountaintop detritus and colluvial deposits found throughout the region are thought to be associated with periglacial activity such as ice wedging. This detritus takes the form of quartzite block fields, talus sheets, rock streams, and tors at summits and along ridgelines (Morgan and others, 2004). These periglacial processes affect rock strength and outcrop stability. Galloway (1961) and Hills (1969) found that in periglacial conditions in Scotland, both granite and quartzite were subjected to frost-shattering, which led to the formation of characteristic landforms such as tors (Eaton and others, 2003a). Driese and others (2005), examining paleosols and floodplain soils in southwestern Virginia, documented a cooler late Pleistocene full-glacial paleoclimate followed by the warmer Holocene interglacial. Clark and Ciolkosz (1988) also confirm the presence of periglacial conditions such as seasonally frozen ground and isolated areas of permafrost from field relations of large-scale microfeatures such as grèzes litées, block fields, and block slopes. They also suggest that paleoperiglacial processes may have been important, geomorphically, at high elevations of the Appalachian Mountains in the Quaternary. During the Holocene, Leigh and Webb (2006) suggest that increased sedimentation rates in the southern

Blue Ridge were due to changes in global paleoclimate that ushered in higher rates and frequency of precipitation in the form of floods and tropical thunderstorms.

Shenandoah National Park region climate.—There are several major influences on climate in Virginia including elevation and the source of moisture driving precipitation. Major winter storms (nor'easters) move northeastward paralleling the Gulf Stream and the coast. As moist air from these storms rises and condenses, the eastern slopes and foothills of the Blue Ridge can receive heavy precipitation (http://www.climate.virginia.edu/description.htm, accessed 14 June 2007) while the western slopes are shadowed and receive less snow and rain. Conversely, other storms move west to east resulting in downsloping and lighter eastern slope precipitation controlled by the high relief of the Appalachian Plateau, and the Blue Ridge. Because of this rain shadow effect, the Shenandoah River Valley is one of the driest areas in the state (http://www.climate.virginia.edu/description.htm, accessed 14 June 2007). Locally, climate is controlled by the complex systems of rivers and valleys that drain the precipitation from the Blue Ridge highlands underlying the Park and modify the pattern of moist airflow. Thunderstorms, which can focus on the high terrain, reach a peak in September, but storms and significant run-off can occur year round with precipitation in the park averaging 100 to 150 cm/yr (http://www.nps.gov/shen/naturescience/weather.htm, accessed on 13 June 2014).

There are significant temperature and precipitation gradients in the park both of which are related to elevation. The mountains in the Shenandoah National Park are usually ~6 °C cooler than the valley below, where mild winters and warm humid summers are the norm. The average annual precipitation at Big Meadows (elevation 1067 m, mean annual temperature, 9 °C) is 132 cm, including ~20 cm of snow/water equivalent (http://www.nps.gov/shen/naturescience/weather.htm, accessed on 13 June 2014). At Luray in the lowland, the mean annual temperature is 12 °C, and average annual precipitation is 91 cm, with <10 cm of snow/water equivalent (http://www.nps.gov/shen/naturescience/weather.htm, accessed on 13 June 2014).

Cosmogenic Nuclides in Erosion Rate Studies

Cosmogenic nuclides, particularly ^{10}Be produced in near-surface rock and sediment, have been used to estimate rates of rock erosion and sediment generation for two decades (Portenga and Bierman, 2011). These nuclides are produced from the interaction of secondary cosmic rays with rock and soil, primarily within the upper two meters of the Earth's surface—the result of spallation, the splitting of target nuclei by incoming, high-energy, fast cosmic ray neutrons (Lal, 1998). The cosmic ray flux is attenuated by rock; thus, ^{10}Be concentrations decrease nearly exponentially with depth. Cosmogenic nuclide production rates are dependent on latitude and altitude (Lal and Peters, 1967). Normalization schemes have been developed (Lal, 1991; Desilets and Zreda, 2000; Dunai, 2000; Lifton, 2000) to account for this effect. When these measured concentrations of cosmogenic isotopes are interpreted using steady-state models, the resulting information suggests the rate at which the landscape has changed over timescales of 10^3 to 10^6 years (Bierman and Nichols, 2004). Of specific utility for this study is the cosmogenic isotope ^{10}Be because it is a long-lived radionuclide and is easily measured in quartz (Gosse and Phillips, 2001; Bierman and others, 2002). Quartz is widely distributed on Earth's surface and can be separated from other minerals because of its low reactivity with various acids (Kohl and Nishiizumi, 1992).

In eroding landscapes, the abundance of ^{10}Be in outcropping rock and soil is proportional to the transit time of rock from depth to surface, allowing erosion rates to be inferred from nuclide concentrations (Lal, 1988). In humid landscapes, rock transitions first to saprolite and then to soil and sediment with the material approaching the lowering surface, all the while accumulating ^{10}Be (Pavich, 1990). As a result, quartz grains in basins that are eroding slowly have a high concentration of ^{10}Be

because they have been exposed to cosmic ray bombardment longer than quartz grains in rapidly eroding basins. Sediment gathered from streams averages ^{10}Be concentration spatially and thus allows calculation of a virtual sediment production rate for the entire basin, rather than for a particular point on the landscape, such as monitored by bedrock samples (Brown and others, 1995; Bierman and Steig, 1996; Granger and others, 1996). The great utility of ^{10}Be-derived erosion rates is that they integrate over millennia, thus masking short-term variability and allowing robust interpretations of geomorphic change over longer time-scales than contemporary data allow (Bierman and Steig, 1996; von Blanckenburg and others, 2004, 2005; Portenga and Bierman, 2011).

Several assumptions underlie the translation of measured isotopic abundances into erosion rates via conceptual and mathematical models (Bierman, 1994). For both sediment and bedrock, it is assumed that the cosmic ray flux is constant over time, and that over the integration period of nuclide build-up, the nuclide production rate is known and on an integrated basis has varied only within the range expressed by the uncertainty of the production rate. For determining bedrock erosion rates, one assumes that there has been no ephemeral shielding from soil, snow, or sediments (Bierman and Nichols, 2004). For sediment, additional assumptions include constant or minimal sediment storage in the sampled basin, steady rates of erosion, adequate mixing of sediment, and homogenous quartz distribution in the drainage basin. Calculation of erosion rates from cosmogenic nuclide data presumes that most chemical weathering occurs within the cosmogenic nuclide production zone, rather than in deep saprolite. In the steeply sloping region we sampled, soils are shallow and thus deep weathering and mass loss by solution at depth is minimal.

METHODS

Sampling Strategy—Basin Selection

The region around and including Shenandoah National Park is ideal for testing the effect of lithology and slope on erosion rates because four distinct lithologies (granite, metabasalt, quartzite, and siliciclastic rocks) crop out in a variety of geomorphic settings. In order to determine whether a relationship between lithology and erosion rate exists, we sampled sediment originating from 41 single-lithology basins. We also collected two temporal replicates of sediment samples. Four initial sample sites were chosen, one for each lithology using 1:24,000 USGS topographic maps and 1:62,500-scale geologic maps of the park. At these first four sample sites, grain-size splits (0.25-0.85 mm, 0.85-2 mm, 2-10 mm, and >10 mm) were collected (11/2005) and later processed separately in order to test the relationship between ^{10}Be concentration and grain size (Brown and others, 1995; Clapp and others, 1997; Clapp and others, 1998; Clapp and others, 2001; Clapp and others, 2002; Matmon and others, 2003a; Matmon and others, 2003b; von Blanckenburg, 2005; Belmont and others, 2006; Sullivan and others, 2006).

Sample sites (figs. 2 and 3) were subsequently selected using ArcGIS to generate a list of single-lithology drainage basins that also considered criteria such as basin size, location, mean slope, and elevation range. These basins were originally delineated using several GIS layers including: USGS 10 m DEM's (Digital Elevation Models) (Chirico and Tanner, 2004) along with bedrock geology that provided an overall characterization of the physiography and principal bedrock formations within the park; National Hydrography Datasets (NHD) provided the stream layer; digital contour maps (DRG, digital raster graphic) were overlaid to provide a visual confirmation of streams and a digitized layer of the National Park boundary. Once the basins were delineated, and the desired criteria were established, we chose specific sample sites so

Fig. 3. Upstream view of Leach Run, Shenandoah National Park (SH-49). This 10.9 km^2 basin drains mix of lithologies and has a basin average slope of 8 degrees.

that basins would be of sufficient size to allow for adequate mixing of sediments within the basin (most > 1 km^2). The basins we selected represented a variety of average slopes, basin sizes, elevations, and lithologies.

The sample sites (fig. 2) were chosen as single-lithology basins where possible. However, in some cases subordinate areas of other rock types crop out. To deal with this, we developed a series of rules that provided upper limits for the surface area of other lithologies in a "single" lithology basin. These rules were based on quartz yields we obtained from sediment as we purified quartz using repeated, dilute HF/HNO_3 etching. We find the following average quartz yields in fluvial sediment from what we know to be single-lithology basins: granite (43%), metabasalt (25%), quartzite (63%), siliciclastic rocks (24%). Basins were identified as single-lithology based on the following rules: metabasalt basins contain $\leq$ 10 percent granite or $\leq$ 20 percent siliciclastic rocks by area and granite basins contain $\leq$ 20 percent metabasalt by area. These cutoffs were chosen in order to ensure that at least 90 percent of the quartz comes from the dominant lithology in the basin.

TABLE 1

Fluvial sample characteristics

Lithology	Number of Samples	Basin Area (km^2)	Slope °	Nested samples
Granite	17 + 3 grain-size splits	~0.4-39.5	11-21	4
Metabasalt*	9 + 3 grain-size splits	~0.1-25.2	8-17	1
Quartzite**	9 + 3 grain-size splits	~0.1-9.4	11-20	0
Siliciclastic	8 + 3 grain-size splits	~0.6-12.7	17-24	1
Multilithology	9	~1.1-18.7	6-20	3
Shenandoah River	1	3305	9	NA
Rappahannock River	1	16.9	8.7	NA

* Includes SH-18 (temporal replicate of SH-02).
** Includes SH-41 (temporal replicate of SH-36).

Field Sampling Methods

Sediment samples were gathered in November 2005, and May and December 2006, from active river or stream channels within or near to the boundaries of the park. Basin size and slope of the sampled basins are a function of geographical location of each lithology (tables 1 and 2). The total area represented by the sampled basins is ~344 km^2 (~43%) of the ~810 km^2 area of the park.

For the quartz-rich lithologies, < 0.5 kg of sample was sufficient to carry out the lab processes to isolate ^{10}Be. Metabasalt, which contained less quartz and more hard-to-remove mafic material, required several times as much sample. Most samples were wet sieved in the field to the 0.25 to 0.85 mm size fraction, the most suitable size for processing in the lab. At the University of Vermont (UVM), samples were oven dried, and if necessary, re-sieved to the 0.25 to 0.85 mm size fraction.

During a subsequent field season (December 2006) we collected five bedrock samples using a hammer and chisel, based on accessibility and occurrence, from each of the four lithologies and from Massanutten Mountain (Silurian sandstone) in the Valley and Ridge Province to the west (table 3). The bedrock samples were taken from non-vegetated outcrops with flat-lying surfaces and were ~2 to 5 cm thick. The bedrock samples were crushed, ground, and sieved to the 0.25 to 0.85 mm size fraction at the UVM.

Laboratory Methods

Quartz was purified at the UVM by ultrasonic and heated-roller etching of samples in hot 6N HCl for two 24-hour periods, followed by three 24-hour etches in dilute HF/HNO_3. After the samples were dry, density separation removed heavy minerals before a final 48-hour etch in dilute HF/HNO_3. For quartz purification purposes, ~60 g of quartzite, ~120 g of granite and siliciclastic rocks and ~180 to 240 g of metabasalt was etched to obtain a 20 to 40 g sample of pure quartz in order to isolate ^{10}Be. The initial four samples with grain-size splits were extracted at the University of Vermont using standard techniques (Bierman and Caffee, 2001). Beryllium isolated from the initial samples was measured using accelerator mass spectrometry (AMS) at Lawrence Livermore National Laboratory (LLNL) with one process blank per seven samples; the average of the UVM blank ratios from the LLNL run was subtracted from the measured ^{10}Be ratios and the uncertainty propagated. The remaining samples were processed to isolate ^{10}Be following procedures based on methods modified from Kohl and Nishiizumi (1992) and Child and others (2000) at the University of Glasgow-Scottish Universities Environmental Research Centre (SUERC) Cosmogenic Nuclide Labora-

TABLE 2

Sample locations

Sample ID	Lithology	Sample Type	Latitude[1]	Longitude	Sample Collection Elevation (m)	USGS[2] 7.5-minute, 1:24,000-scale Quadrangles	Stream/River/Bedrock
SH-01 (0.25-0.85 mm)	Granite	fluvial sediment	38.57121	-78.28735	283	Old Rag Mountain	Hughes
SH-01 (0.85-2 mm)	Granite	fluvial sediment	--	--	--	--	--
SH-01 (2-10 mm)	Granite	fluvial sediment	--	--	--	--	--
SH-01 (>10 mm)	Granite	fluvial sediment	--	--	--	--	--
SH-07	Granite	fluvial sediment	38.58155	-78.41427	475	Big Meadows	Buracker Hollow
SH-08	Granite	fluvial sediment	38.63410	-78.39168	354	Luray	South Fork Dry Run
SH-10	Granite	fluvial sediment	38.65694	-78.28215	375	Thornton Gap	Thornton
SH-11	Granite	fluvial sediment	38.65282	-78.24489	226	Washington	Thornton
SH-12	Granite	fluvial sediment	38.61456	-78.25663	293	Old Rag Mountain	Hazel
SH-13	Granite	fluvial sediment	38.54308	-78.27286	223	Old Rag Mountain	Rosson Hollow Run
SH-14	Granite	fluvial sediment	38.52742	-78.27909	218	Old Rag Mountain	Ragged Run
SH-15	Granite	fluvial sediment	38.52129	-78.29047	232	Old Rag Mountain	Popham Run
SH-21	Granite	fluvial sediment	38.64484	-78.36921	402	Thornton Gap	North Fork Dry Run
SH-22	Granite	fluvial sediment	38.61039	-78.41763	329	Big Meadows	Tributary of East Hawksbill Creek
SH-45	Granite	fluvial sediment	38.52343	-78.26451	195	Old Rag Mountain	Dulaney Hollow
SH-46	Granite	fluvial sediment	38.64164	-78.24595	232	Washington	Jenkins Hollow
SH-47	Granite	fluvial sediment	38.64702	-78.20854	183	Washington	Beaverdam Creek
SH-50	Granite	fluvial sediment	38.81878	-78.20828	354	Chester Gap	Lands Run Tributary
SH-51	Granite	fluvial sediment	38.79600	-78.23921	317	Chester Gap	Phils Arm Run
SH-52	Granite	fluvial sediment	38.81109	-78.23393	287	Chester Gap	Gooney Run
SH-59	Granite	bedrock	38.63790	-78.30890	835	Thornton Gap	bedrock
SH-02 (0.25-0.85 mm)	Metabasalt	fluvial sediment	38.66350	-78.35550	390	Thornton Gap	Pass Run
SH-02 (0.85-2 mm)	Metabasalt	fluvial sediment	--	--	--	--	--
SH-02 (2-10 mm)	Metabasalt	fluvial sediment	--	--	--	--	--
SH-02 (>10 mm)	Metabasalt	fluvial sediment	--	--	--	--	--
SH-05	Metabasalt	fluvial sediment	38.75965	-78.29867	762	Bentonville	Jeremys Run
SH-09	Metabasalt	fluvial sediment	38.69730	-78.32236	695	Thornton Gap	Rocky Branch
SH-16	Metabasalt	fluvial sediment	38.54164	-78.35171	360	Old Rag Mountain	White Oak Run
SH-18*	Metabasalt	fluvial sediment	38.66361	-78.35552	384	Thornton Gap	Pass Run - Shenks Hollow
SH-19	Metabasalt	fluvial sediment	38.47084	-78.49769	451	Fletcher	East Branch Naked Creek
SH-25	Metabasalt	fluvial sediment	38.14798	-78.74870	341	Browns Cove	North Fork Moormans River
SH-26	Metabasalt	fluvial sediment	38.29310	-78.62078	610	Swift Run	Ivy Creek - Fork Hollow
SH-40	Metabasalt	fluvial sediment	38.23854	-78.69121	512	Browns Cove	Doyles
SH-58	Metabasalt	bedrock	38.70190	-78.32570	860	Thornton Gap	bedrock
SH-03 (0.25-0.85 mm)	Quartzite	fluvial sediment	38.3617	-78.6540	344	McGaheysville	Gap Run
SH-03 (0.85-2 mm)	Quartzite	fluvial sediment	--	--	--	--	--
SH-03 (2-10 mm)	Quartzite	fluvial sediment	--	--	--	--	--

TABLE 2
continued

Sample ID	Lithology	Sample Type	Latitude[1]	Longitude	Sample Collection Elevation (m)	USGS[2] 7.5-minute, 1:24,000-scale Quadrangles	Stream/River/Bedrock
SH-03 (>10 mm)	Quartzite	fluvial sediment	--	--	--	--	--
SH-20	Quartzite	fluvial sediment	38.3568	-78.6621	341	McGaheysville	Walls Run
SH-29	Quartzite	fluvial sediment	38.1092	-78.8283	469	Waynesboro East	unnamed
SH-30	Quartzite	fluvial sediment	38.1782	-78.7893	604	Crimora	Meadow Run - Rip Rap Hollow
SH-32	Quartzite	fluvial sediment	38.3101	-78.7269	378	McGaheysville	Hangmans Run Tributary
SH-34	Quartzite	fluvial sediment	38.1728	-78.8094	488	Crimora	Meadow Run Tributary
SH-35	Quartzite	fluvial sediment	38.1759	-78.8071	524	Crimora	Meadow Run Tributary
SH-36	Quartzite	fluvial sediment	38.1775	-78.8057	536	Crimora	Meadow Run Tributary
SH-41**	Quartzite	fluvial sediment	38.1776	-78.8059	564	Crimora	Meadow Run Tributary
SH-55	Quartzite	bedrock	38.29780	-78.72540	518	McGaheysville	bedrock
SH-04 (0.25-0.85 mm)	Siliciclastic	fluvial sediment	38.19886	-78.79376	427	Crimora	Paine Run
SH-04 (0.85-2 mm)	Siliciclastic	fluvial sediment	--	--	427	--	--
SH-04 (2-10 mm)	Siliciclastic	fluvial sediment	--	--	427	--	--
SH-04 (>10 mm)	Siliciclastic	fluvial sediment	--	--	427	--	--
SH-06	Siliciclastic	fluvial sediment	38.67620	-78.38344	299	Luray	Britton Hollow (tributary of Pass Run)
SH-27	Siliciclastic	fluvial sediment	38.09966	-78.80402	475	Waynesboro East	Tributary of Saw Mill Run
SH-28	Siliciclastic	fluvial sediment	38.09913	-78.80430	457	Waynesboro East	Saw Mill Run
SH-37	Siliciclastic	fluvial sediment	38.25227	-78.74652	463	McGaheysville	Madison Run
SH-39	Siliciclastic	fluvial sediment	38.22154	-78.78121	512	Crimora	Stull Run
SH-42	Siliciclastic	fluvial sediment	38.15973	-78.78496	640	Crimora	unnamed
SH-54	Siliciclastic	fluvial sediment	38.28971	-78.72392	503	McGaheysville	Lower Lewis Run
SH-57	Siliciclastic	bedrock	38.70360	-78.72540	811	Thornton Gap	bedrock
SH-17	Multilithology	fluvial sediment	38.77959	-78.36560	195	Bentonville	Dry Run
SH-23	Multilithology	fluvial sediment	38.86900	-78.17800	285	Chester Gap	Happy Creek
SH-24	Multilithology	fluvial sediment	38.16600	-78.74500	459	Browns Cove	Moormons R. N. Fork (trib of)
SH-31	Multilithology	fluvial sediment	38.16031	-78.80311	469	Crimora	Meadow Run
SH-33	Multilithology	fluvial sediment	38.31137	-78.72635	360	McGaheysville	Hangmans Run
SH-38	Multilithology	fluvial sediment	38.25673	-78.76888	415	Grottoes	Madison Run
SH-43	Multilithology	fluvial sediment	38.36257	-78.57390	472	Swift Run	Swift Run
SH-44	Multilithology	fluvial sediment	38.34114	-78.45703	259	Stannardsville	unnamed
SH-48	Multilithology	fluvial sediment	38.83800	-78.10600	213	Flint Hill	Rappahanock
SH-49	Multilithology	fluvial sediment	38.92655	-78.17554	165	Front Royal	Leach Run
SH-56	Multilithology	fluvial sediment	38.53189	-78.60295	256	Stanley	Shenandoah
SH-53	Sandstone	bedrock	38.65200	-78.60200	692	Hamburg	Massanutten Ridge

[1] Coordinate System - NAD 83 using a Garmin 12 GPS unit.
[2] United States Geological Survey.
* Temporal replication of SH-02.
** Temporal replication of SH-36.

TABLE 3

Bedrock samples ^{10}Be concentrations and model erosion rates

Sample ID	Lithology	SUERC[1] ID #[2]	Sample thickness (cm)	^{10}Be Concentration (x 10^5 atoms/gram)[3*]	^{10}Be Model Erosion Rate (m/My)[4*]
SH-53	Sandstone	B2268	2.5	17.8 ± 0.32	2.82 ± 0.3
SH-55	Quartzite	B2272	4.5	22.4 ± 0.37	1.78 ± 0.2
SH-57	Siliciclastic	B2260	2.5	5.91 ± 0.11	10.7 ± 0.9
SH-58	Metabasalt	B2273	5.0	6.01 ± 0.19	10.9 ± 0.9
SH-59	Granite	B2274	2.5	9.65 ± 0.17	6.35 ± 0.5

[1] SUERC - Scottish Universities Environmental Research Centre, Accelerator Mass Spectrometry Laboratory.

[2] SUERC ID # -

[3] Normalized to NIST (SRM4325) assuming $^{10/9}Be$ ratio for standard = 3.06×10^{11} including blank corrections; uncertainty is counting statistics with uncertainty in carrier concentration (Be 2%) added quadratically.

[4] Using density of 2.7 g cm^{-3} and attenuation coefficient of 160 g/cm^2.

* one σ analytical uncertainty.

tory (CNL) (http://web2.ges.gla.ac.uk/~dfabel/CN_intro.html) at SUERC (http://www.gla.ac.uk/research/az/suerc/) in East Kilbride, Scotland. The ^{10}Be isolated from the remaining samples was then measured using AMS at the SUERC Accelerator Mass Spectrometry Laboratory. Process blanks were run with every fifteen samples and average blank $^{10}Be/^{9}Be$ ratios were subtracted from measured ratios of samples. In most cases, blank ratios made up at most several percent of measured ratios on samples.

Calculation of Erosion Rates from ^{10}Be and Data Analysis

Beryllium isotopic ratios of the initial four samples (grain-size splits) were normalized using standards developed by Nishiizumi assuming a ^{10}Be half-life of 1.5 My (KNSTD 3110, $^{10/9}Be = 3.15 \times 10^{12}$; Nishiizumi and others, 2007). The remaining samples were analyzed at SUERC where results are expressed in units of a National Institute of Standards and Technology standard reference material (NIST SRM 4325). These are propagated with a half-life-matching SRM $^{10/9}Be$ ratio of 3.06×10^{11} for consistency with the original values (but see Nishiizumi and others, 2007).

Erosion rates were calculated using the CRONUS calculator (Balco and others, 2008) using methods described in Portenga and Bierman (2011) and the appropriate standard values. Erosion rates and ^{10}Be concentrations were analyzed with respect to lithology, slope, basin area, grain size, and aspect.

DATA

Samples of rock and fluvial sediment from Shenandoah National Park and adjacent Massanutten Mountain contain high concentrations of *in situ* produced ^{10}Be indicating stable, slowly eroding ridgelines.

The five bedrock samples have an average ^{10}Be concentration of $12.4 \pm 7.4 \times 10^5$ atoms/g (one standard deviation). Erosion rates for these samples range from 2.8 to 11 m/My (table 3).

Grain-size specific ^{10}Be analysis of four river sediment samples showed no reproducible trend of concentration with grain size (table 4, fig. 4). The ^{10}Be concentrations (table 4) for these grain-size splits indicate that within each lithology there are similar average cosmic-ray dosing histories. ^{10}Be concentrations (table 4) in granite and

TABLE 4

Fluvial samples ^{10}Be concentrations and erosion rates

Sample ID	Lithology	CAMS #[1]/ SUERC ID #[2]	Basin Area (km^2)	Effective Basin Elevation (m)[3]	Slope °	^{10}Be Concentration ($x10^5$ atoms/gram)[4†]	^{10}Be Model Erosion Rate (m/My)[5†]	Drainage Direction	Nesting Level
SH-01 (0.25-0.85 mm)	Granite	BE22557	39.49	717	16.8	3.48 ± 0.10	18.0 ± 1.4	East	0
SH-01 (0.85-2 mm)	Granite	BE22558	--	--	16.8	3.42 ± 0.13	--		
SH-01 (2-10 mm)	Granite	BE22559	--	--	16.8	3.06 ± 0.14	--		
SH-01 (>10 mm)	Granite	BE22560	--	--	16.8	2.29 ± 0.07	--		
SH-07	Granite	B2189	6.40	831	21.0	5.03 ± 0.10	13.1 ± 1.0	West	0
SH-08	Granite	B2190	4.58	732	18.0	3.26 ± 0.07	19.5 ± 1.5	West	0
SH-10	Granite	B2241	14.09	659	16.7	3.62 ± 0.08	16.6 ± 1.3	East	0
SH-11	Granite	B2194	24.31	569	16.2	3.60 ± 0.09	15.6 ± 1.2	East	1
SH-12	Granite	B2195	14.19	702	15.1	4.28 ± 0.10	14.2 ± 1.1	East	0
SH-13	Granite	B2242	1.79	321	10.8	4.55 ± 0.09	10.0 ± 0.8	East	0
SH-14	Granite	B2196	0.96	470	15.7	3.36 ± 0.14	15.7 ± 1.3	East	1
SH-15	Granite	B2198	5.97	440	16.4	4.23 ± 0.08	11.9 ± 0.9	East	0
SH-21	Granite	B2202	5.65	707	19.2	4.58 ± 0.09	13.3 ± 1.0	West	0
SH-22	Granite	B2244	2.66	507	14.3	6.55 ± 0.12	7.7 ± 0.6	West	0
SH-45	Granite	B2235	4.14	258	11.3	4.88 ± 0.11	8.8 ± 0.7	East	0
SH-46	Granite	B2236	1.58	442	17.0	2.76 ± 0.07	19.1 ± 1.4	East	0
SH-47	Granite	B2254	12.48	304	11.0	3.94 ± 0.08	11.6 ± 0.9	East	1
SH-50	Granite	B2265	0.35	508	15.0	7.14 ± 0.13	7.0 ± 0.6	West	0
SH-51	Granite	B2266	4.51	562	15.1	5.22 ± 0.10	10.4 ± 0.8	West	0
SH-52	Granite	B2267	22.91	583	14.6	4.88 ± 0.11	11.3 ± 0.9	West	1
SH-02 (0.25-0.85 mm)	Metabasalt	BE22589	2.81	607	11.9	10.23 ± 0.29	5.0 ± 0.4	West	0
SH-02 (0.85-2 mm)	Metabasalt	BE22590	--	--	11.9	8.73 ± 0.27	--		
SH-02 (2-10 mm)	Metabasalt	BE22591	--	--	11.9	7.90 ± 0.21	--		
SH-02 (>10 mm)	Metabasalt	BE22592	--	--	11.9	7.89 ± 0.25	--		
SH-05	Metabasalt	B2188	1.52	819	8.2	15.13 ± 0.21	3.8 ± 0.3	West	0
SH-09	Metabasalt	B2193	0.06	804	14.4	8.77 ± 0.19	7.0 ± 0.6	West	0
SH-16	Metabasalt	B2199	13.80	890	13.7	3.33 ± 0.07	21.3 ± 1.6	East	0
SH-18*	Metabasalt	B2200	2.83	605	11.9	10.99 ± 0.20	4.6 ± 0.4	West	0
SH-19	Metabasalt	B2201	11.49	836	15.9	5.35 ± 0.10	12.3 ± 1.0	West	0
SH-25	Metabasalt	B2205	25.22	714	17.3	7.29 ± 0.33	7.9 ± 0.7	East	1
SH-26	Metabasalt	B2264	2.48	797	13.9	6.26 ± 0.12	10.0 ± 0.8	East	0
SH-40	Metabasalt	B2231	3.37	815	15.1	8.24 ± 0.14	7.5 ± 0.6	East	0
SH-03 (0.25-0.85 mm)	Quartzite	BE21899	9.43	502	15.4	7.44 ± 0.20	6.6 ± 0.6	West	0
SH-03 (0.85-2 mm)	Quartzite	BE21900	--	--	15.4	5.84 ± 0.16	--		
SH-03 (2-10 mm)	Quartzite	BE21901	--	--	15.4	5.06 ± 0.17	--		
SH-03 (>10 mm)	Quartzite	BE22593	--	--	15.4	5.95 ± 0.16	--		
SH-20	Quartzite	B2243	1.61	569	16.8	8.36 ± 0.16	6.1 ± 0.5	West	0
SH-29	Quartzite	B2207	0.01	584	14.0	12.63 ± 0.19	3.8 ± 0.3	West	0
SH-30	Quartzite	B2211	0.80	778	15.3	9.34 ± 0.15	6.3 ± 0.5	West	0
SH-32	Quartzite	B2213	1.05	472	10.8	10.86 ± 0.17	4.1 ± 0.4	West	0

TABLE 4
continued

Sample ID	Lithology	CAMS #[1]/ SUERC ID #[2]	Basin Area (km^2)	Effective Basin Elevation (m)[3]	Slope °	^{10}Be Concentration ($x10^5$ atoms/gram)[4†]	^{10}Be Model Erosion Rate (m/My)[5†]	Drainage Direction	Nesting Level
SH-34	Quartzite	B2224	0.40	616	17.9	3.91 ± 0.08	14.7 ± 1.1	West	0
SH-35	Quartzite	B2225	0.04	555	16.6	9.37 ± 0.33	5.3 ± 0.5	West	0
SH-36	Quartzite	B2226	0.19	645	19.9	6.14 ± 0.16	9.1 ± 0.7	West	0
SH-41**	Quartzite	B2250	0.18	639	19.8	7.17 ± 0.14	7.6 ± 0.6	West	0
SH-04 (0.25-0.85 mm)	Siliciclastic	BE22525	12.71	656	21.3	4.04 ± 0.13	14.6 ± 1.2	West	0
SH-04 (0.85-2 mm)	Siliciclastic	BE22526	--	--	21.3	3.69 ± 0.12	--		
SH-04 (2-10 mm)	Siliciclastic	BE22527	--	--	21.3	4.09 ± 0.13	--		
SH-04 (>10 mm)	Siliciclastic	BE22528	--	--	21.3	5.58 ± 0.17	--		
SH-06	Siliciclastic	B2240	1.47	452	18.0	7.80 ± 0.15	6.0 ± 0.5	West	0
SH-27	Siliciclastic	B2249	3.44	636	16.6	10.06 ± 0.15	5.2 ± 0.4	West	0
SH-28	Siliciclastic	B2206	5.70	636	16.6	9.35 ± 0.14	5.6 ± 0.5	West	1
SH-37	Siliciclastic	B2228	1.59	620	19.6	6.99 ± 0.12	7.7 ± 0.6	West	0
SH-39	Siliciclastic	B2230	3.06	756	24.4	6.96 ± 0.36	8.6 ± 0.8	West	0
SH-42	Siliciclastic	B2252	0.58	788	19.5	4.46 ± 0.09	14.4 ± 1.1	West	0
SH-54	Siliciclastic	B2492	1.78	679	22.4	4.19 ± 0.10	14.3 ± 1.1	West	0
SH-17	Multilithology	B2262	9.28	489	15.0	10.56 ± 0.20	4.4 ± 0.4	West	0
SH-23	Multilithology	B2247	18.73	497	12.5	3.33 ± 0.07	16.2 ± 1.2	West	0
SH-24	Multilithology	B2248	3.65	730	19.7	5.23 ± 0.13	11.6 ± 0.9	East	0
SH-31	Multilithology	B2212	8.47	728	18.4	8.19 ± 0.13	7.0 ± 0.6	West	1
SH-33	Multilithology	B2214	1.11	467	10.6	10.59 ± 0.16	4.3 ± 0.4	West	1
SH-38	Multilithology	B2229	15.12	647	19.2	6.71 ± 0.12	8.3 ± 0.7	West	1
SH-43	Multilithology	B2253	2.12	640	13.9	4.24 ± 0.09	13.7 ± 1.1	West	0
SH-44	Multilithology	B2232	1.26	269	5.7	5.06 ± 0.12	8.5 ± 0.7	East	0
SH-48	Multilithology	B2255	16.85	403	10.6	3.80 ± 0.08	13.1 ± 1.0	East	0
SH-49	Multilithology	B2237	10.88	277	8.0	12.42 ± 0.20	3.0 ± 0.3	West	0
SH-56	Multilithology	B2256	3305.62	634	8.7	8.14 ± 0.15	6.6 ± 0.5	West	2

[1] CAMS (Center for Accelerator Mass Spectrometry) # for samples SH-01-SH-04.
[2] SUERC (Scottish Universities Environmental Research Centre, Accelerator Mass Spectrometry Laboratory) # for samples SH-05-SH-59).
[3] Calculated for entry into CRONUS as per Portenga and Bierman (2011).
[4] At Lawrence Livermore National Laboratory, normalized to KNSTD standards prepared by K. Nishizumi. At SUERC, normalized to NIST (SRM4325) assuming $^{10/9}Be$ ratio for standard = 3.06×10^{-11}. Including blank corrections; error is counting statistics with uncertainty in carrier concentration (Be 2%) added quadratically. Using density of 2.7 g cm^{-3} and attenuation coefficient of 160 g cm^{-2}.
[5] Calculated using CRONUS (Portenga and Bierman, 2011).
† one σ analytical error.
* Temporal replication of SH-02.
** Temporal replication of SH-36.

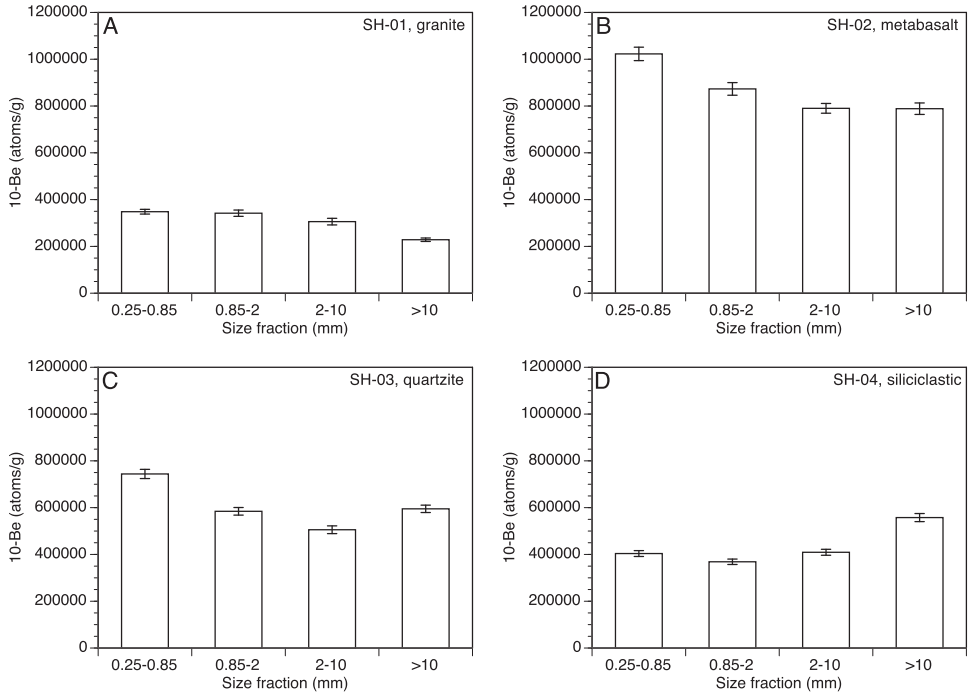

Fig. 4. Measured ^{10}Be concentrations by grain-size. (A) granite, (B) metabasalt, (C) quartzite, (D) siliciclastic rocks. Error bars are one standard deviation analytical error.

metabasalt samples exhibit monotonic decreases with increasing grain size (figs. 4A and 4B). Quartzite samples exhibit a monotonic decrease through increasing grain-size except for >10 mm fraction (fig. 4C). Sediment from siliciclastic basins has no discernable pattern (fig. 4D).

Fluvial samples (n = 54) (tables 2 and 4), collected from streams draining the highlands contain 2.29 to 15.1 $\times$ 10^5 atoms/g ^{10}Be. Considering the data by lithology, ^{10}Be concentration ranges were: granite, 2.29 to 7.14 $\times$ 10^5 atoms/g; metabasalt, 3.33 to 15.1 $\times$ 10^5 atoms/g; quartzite, 3.91 to 12.6 $\times$ 10^5 atoms/g, and siliciclastic rocks, 3.69–10.1 $\times$ 10^5 atoms/g (table 4). Multilithology samples (basins containing sediment derived from more than one lithology) have ^{10}Be concentrations (3.33-12.4 $\times$ 10^5 atoms/g) similar to range of ^{10}Be concentration for all lithologies (2.29-15.1 $\times$ 10^5 atoms/g).

The inferred erosion rates for all basins sampled range from 3.0 to 21 m/My (table 4). The area-weighted mean erosion rate for all basins in the park is 12.2 m/My (n = 53). By lithology, the erosion rate ranges are: granite, 7.0 to 20 m/My (n = 17); metabasalt, 3.8 to 21 m/My (n = 9); quartzite, 3.8 to 15 m/My (n = 9); and siliciclastic rocks, 5.2 to 15 m/My (n = 8). The range of erosion rates for multilithology basins (n = 10) is 3.0 to 16 m/My. The Shenandoah River basin (3305 km^2) is eroding at 6.6 m/My. The measured concentrations of ^{10}Be in temporal replicates (SH-18 and SH-02, metabasalt; SH-41 and SH-36, quartzite) collected ~6 months apart and within several hundred meters of the original collection site agree well (table 4, 10.99 $\pm$ 0.20 versus 10.23 $\pm$ 0.29 and 7.17 $\pm$ 0.14 versus 6.14 $\pm$ 0.16 $\times$ 10^5 atoms/g of quartz)$^{-1}$) indicating the range of variability in isotope concentration over this time period.

DISCUSSION

New cosmogenic nuclide data clearly indicate that over millennial time scales, outcrops and drainage basins in the Blue Ridge around Shenandoah National Park are eroding slowly, on the order of meters to at most a few tens of meters per million years. This finding is in good agreement with other cosmogenic (Matmon and others, 2003a; Matmon and others, 2003b; Reuter, ms, 2005; Ward and others, 2005; Sullivan and others, 2006; Whitten, ms, 2009; Trodick and others, 2010; Portenga and others, 2013) and thermochronologic studies (Roden, 1991; Blackmer and others, 1994; Boettcher and Milliken, 1994; Naeser and others, 2004; Spotila and others, 2004; Naeser and others, 2005; Reed, 2005; Naeser and others, 2006a; Naeser and others, 2006b) in the Appalachian Mountains, which all suggest erosion rates of at most a few tens of meters per million years.

Comparing Erosion Rates

Slope.—Erosion rate and slope appear to be positively related in the areas around and including Shenandoah National Park (fig. 5) similar to findings elsewhere in the Appalachians (Matmon and others, 2003a; Matmon and others, 2003b; Reuter, ms, 2005; Sullivan and others, 2006). Considering all Shenandoah drainage basin samples after averaging replicates, there is a weak and positive correlation between erosion rate and slope ($p = 0.03$, $R^2 = 0.09$). When the data are considered by lithology, only quartzite and granite have slope-erosion rate regressions with p values < 0.10.

Area.—There is no significant relationship between erosion rate and basin area for any single lithology, indicating that basin scale does not influence erosion rate (fig. 6). There is a weak positive ($R^2 = 0.15$) and statistically significant relationship ($p = 0.005$) between erosion rate and basin area for all samples (table 4, fig. 6F) that is likely an artifact of basin size and sampling strategy. The erosion rate-area relationship becomes statistically insignificant if the quartzite basins (small and slowly eroding) and the granitic basins (larger and more rapidly eroding) are removed from the regression. The variability of erosion rates does not decrease with increasing basin area likely because most basins are headwaters.

The are no statistically significant regressions ($p \leq 0.10$) between slope and basin area, likely the result of the study area's morphology, an elongate ridgeline with sloping basins to the east and west. Even the largest sampled basins, with the exception of the 3305 km^2 Shenandoah River watershed, did not contain significant lowland areas.

Grain size.—Grain-size specific cosmogenic analysis of four sediment samples showed no consistent trend of concentration (fig. 4) but did indicate ~26 to 34 percent differences on average between the sand-fraction (250-850 mm) we analyzed and larger grain sizes. Such differences may reflect different source areas or processes delivering different grain sizes to the channels (Brown and others, 1995; Matmon and others, 2003a; Matmon and others, 2003b). Because the differences in nuclide concentrations between grain sizes are not systematic and in most cases are not large, they may add noise but do not bias the results.

Lithology.—In the Shenandoah National Park area, there are few statistically significant relationships between landscape-scale metrics and fluvial erosion rates. Of the four lithologies tested, only the erosion rates of drainage basins underlain by quartzite (slower) and granite (more rapid) were separable using the Tukey-Kramer HSD test ($\alpha = 0.05$, fig. 7). The stability or resistance to weathering of quartzite, likely due to its high silica content (Goudie 1995), is well known and supported by field studies (Merschat, 1997) and at the landscape scale using cosmogenic nuclides by Bierman and others (1998). The lack of a more definitive relationship between basin-scale erosion rates and lithology echoes previous work in Namibia (Bierman and

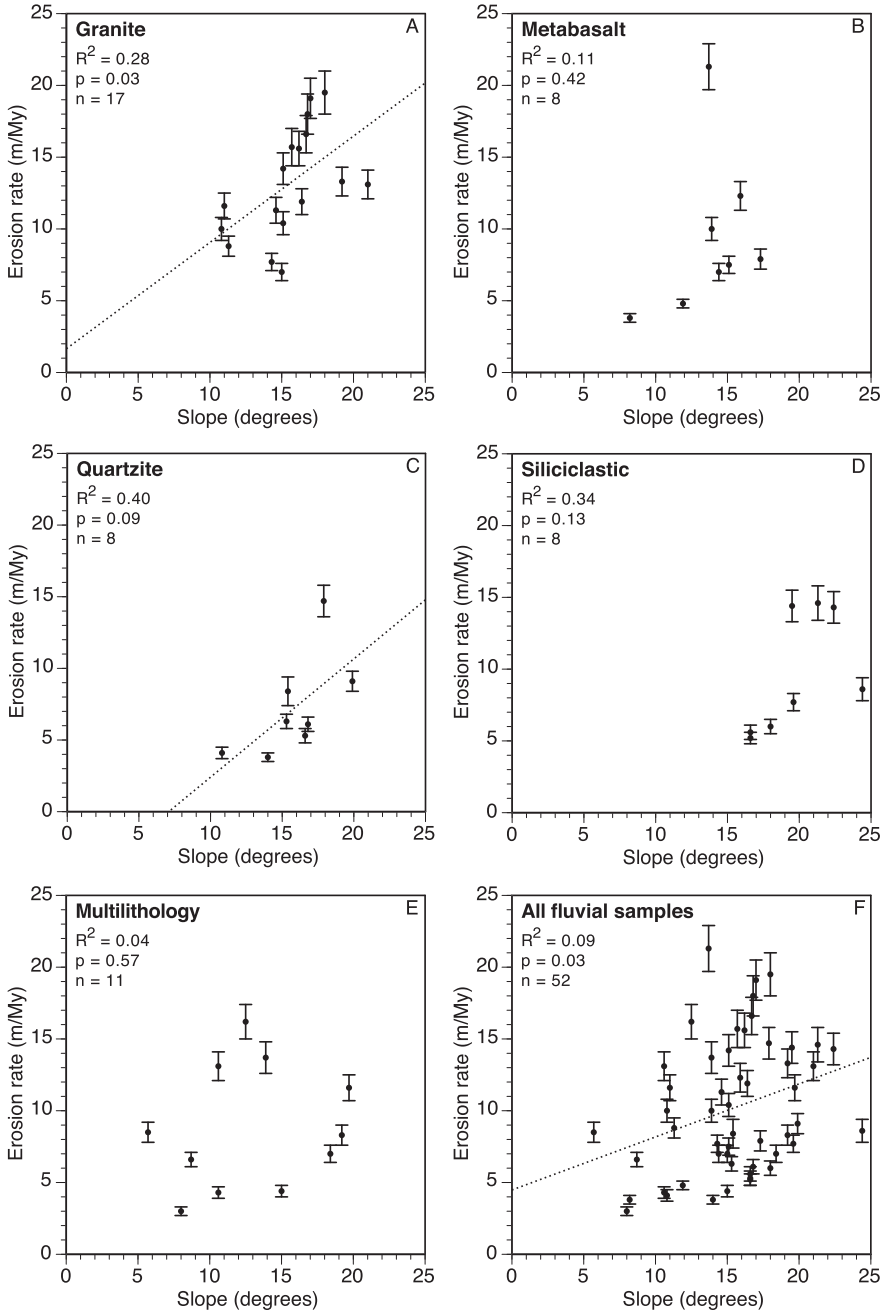

Fig. 5. Erosion rate versus slope relationships. (A) granite, (B) metabasalt, (C) quartzite, (D) siliciclastic rocks, (E) multilithology, (F) all fluvial samples. Error bars are one standard deviation analytical uncertainty. Trend lines shown only for statistically significant ($p < 0.1$) relationships.

Caffee, 2001), the Great Smoky Mountains (Matmon and others, 2003a; Matmon and others, 2003b), and the Susquehanna River Basin (Reuter, ms, 2005).

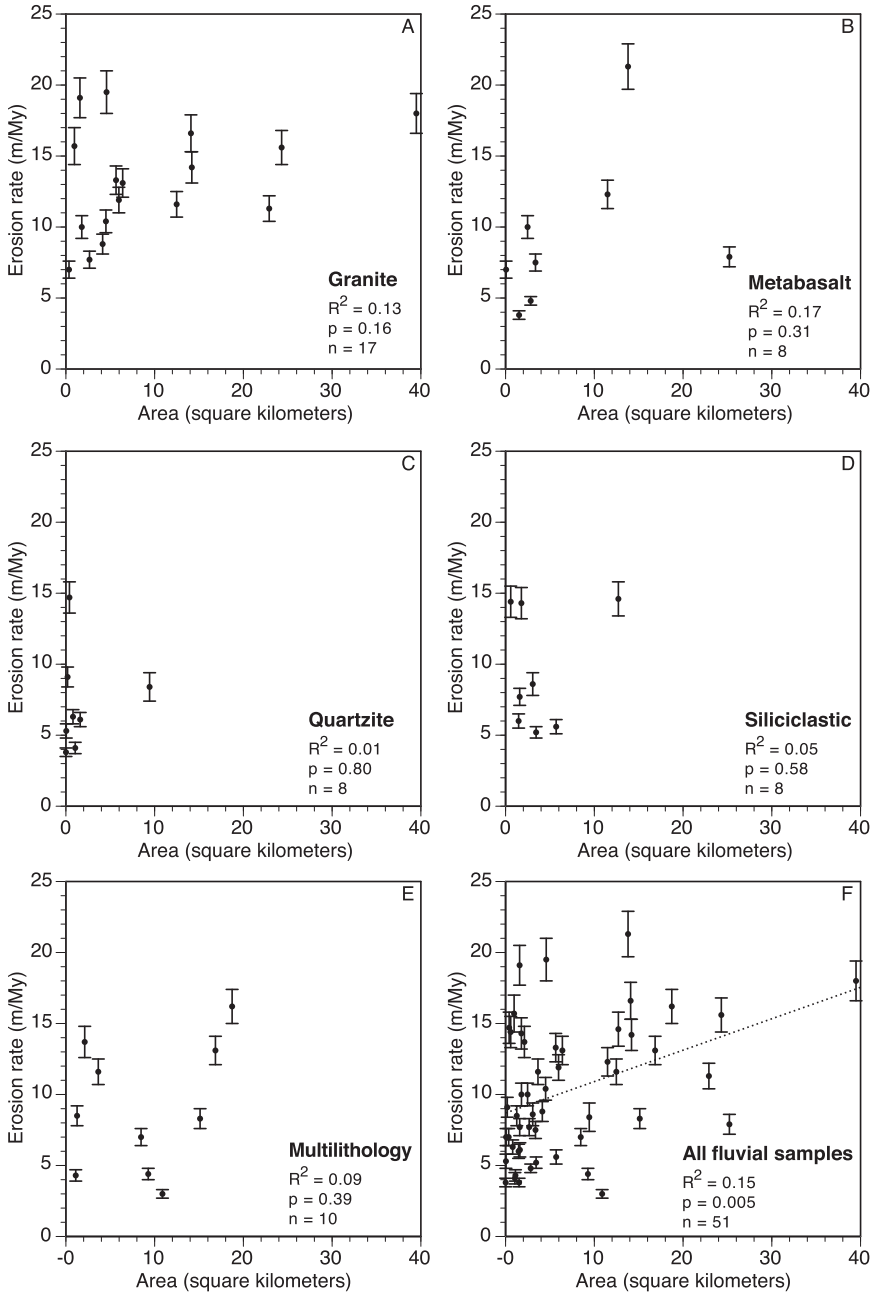

Fig. 6. Basin area and erosion rate relationships (A) Granite, (B) Metabasalt, (C) Quartzite, (D) Siliciclastic rocks, (E) Multilithology, SH-56, Shenandoah River basin not shown, (F) All fluvial samples. Error bars are one standard deviation. Trend lines shown only for statistically significant ($p < 0.1$) relationship.

Bedrock and sediment.—Bedrock samples (n = 5) that we collected in and around Shenandoah National Park indicate that rock outcrops are eroding slowly (table 3).

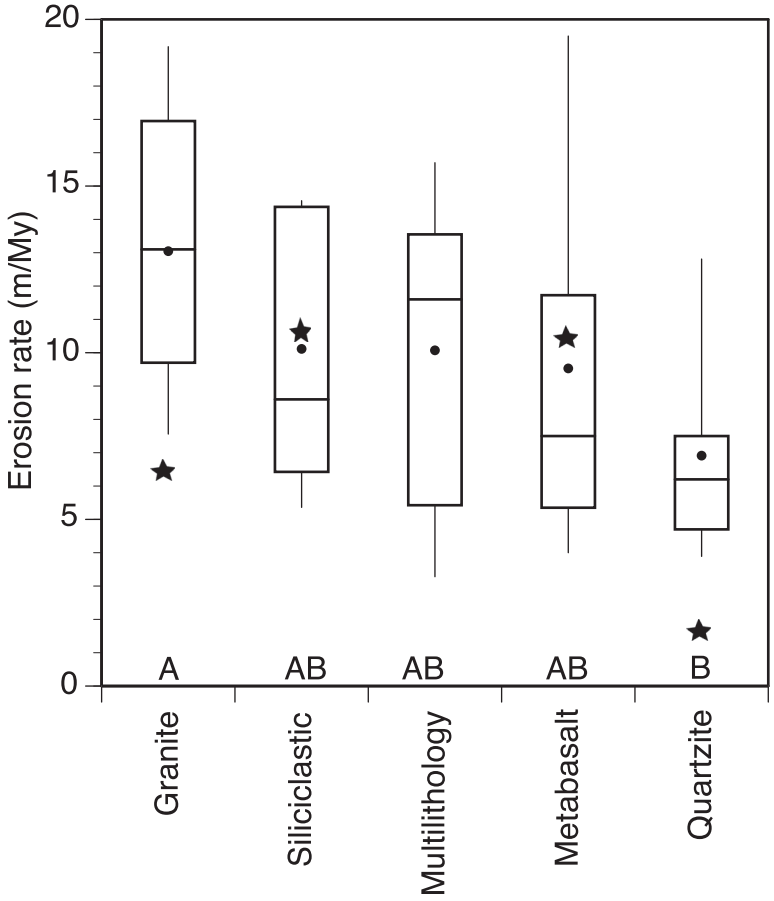

Fig. 7. Boxplot of fluvial and bedrock erosion rates by lithology. Lower line of the box is the 25th percentile, middle line is the median, and the upper line is the 75th percentile. Whiskers are 10th percentile and 90th percentiles. Circles are the mean fluvial erosion rates; stars are bedrock erosion rates. Letters indicate subpopulations that are statistically indistinguishable.

The central tendency and range of our results is similar to measurements made by others. For example, Whitten (ms, 2009) estimates a bare rock erosion rate average of 9.7 m/My based on ^{10}Be measurements made on samples collected from 20 outcrops in Shenandoah National Park. Portenga and others (2013) used ^{10}Be to estimate erosion rates for bedrock exposed on Massanutten Ridge to the west of Shenandoah National Park (1.8-25 m/My, n = 9) and north of Shenandoah near Catoctin and Harpers Ferry (n = 15, ranging 1.0-13 m/My).

The range of bedrock (1.8-11 m/My, n = 5) and basin-scale erosion rates after averaging replicates (3.0-21 m/My, n = 52) mostly overlap, with the exception of one sampled quartzite outcrop which is eroding more slowly than any of the sampled drainage basins (fig. 7). Although the number of bedrock samples in this study is limited (n = 5) and the variability in erosion rates too great to provide much statistical power, bedrock outcrops are eroding more slowly on average ($\mu = 6.5 \pm 4.3$ m/My, n = 5) than drainage basins ($\mu = 10.2 \pm 4.6$ m/My, n = 52). Using the Tukey-Kramer HSD test, the populations are different only at $\alpha = 0.1$. Such a discrepancy between bedrock and fluvial erosion rates has been noted elsewhere (Bierman and Caffee,

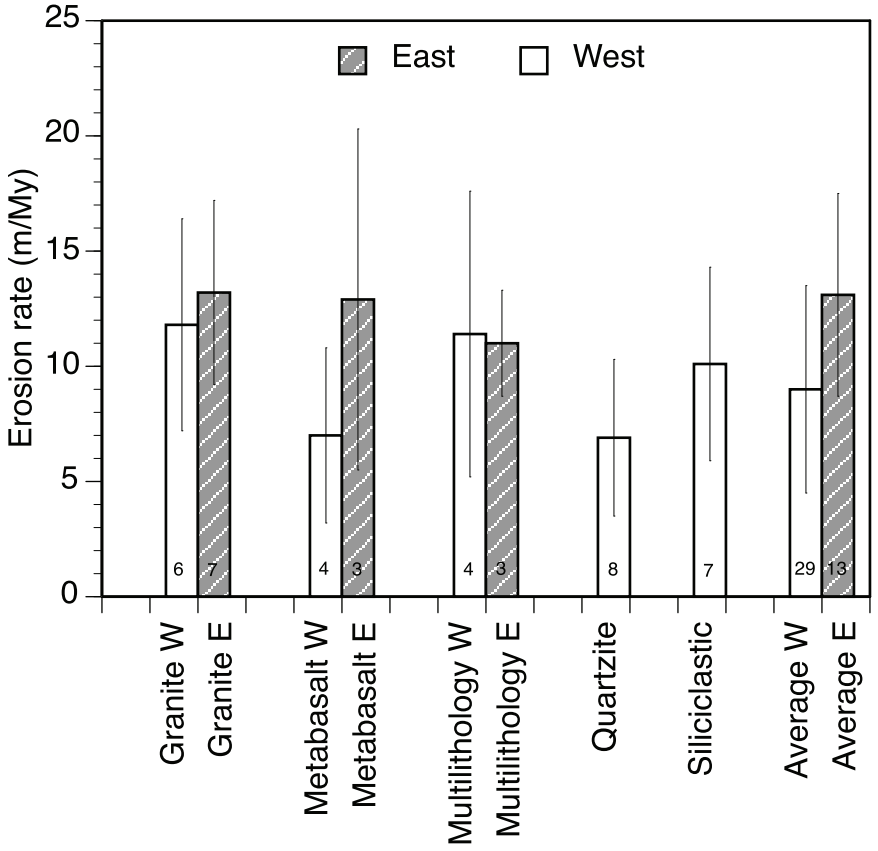

Fig. 8. Histogram of basin-scale erosion rate dependence on aspect by lithology and for all samples. Numbers in the bars are count of samples collected in each lithology. Temporal replicates averaged and only data from non-nested headwater basins are plotted. Error bars represent one standard deviation. Data for basins to the east of the divide are shown by hatched bars.

2001; Clapp and others, 2001; Clapp and others, 2002; Reuter, ms, 2005) and likely reflects the increased efficacy of bedrock to saprolite conversion under a soil mantle (Heimsath and others, 1999; Heimsath and others, 2000; Heimsath and others, 2001). Sampling bedrock outcrops near and along ridgelines biases sample collection toward the most high-standing topography, and thus perhaps some of the most stable elements of the landscape.

East versus West erosion rates.—Erosion rates appear to be different on either side of the drainage divide (fig. 8 and table 5). For example, both granite and metabasalt basins on the eastern side of the divide erode more rapidly on average than basins in the same lithology on the western side of the divide. Considering only non-nested, headwater basins, erosion rates on the eastern side of the divide are faster ($\mu = 13.1 \pm 4.4$ m/My, n = 13) than those on the west ($\mu = 9.0 \pm 4.5$ m/My, n = 29). Using the Tukey-Kramer HSD test, the populations are different at $\alpha = 0.01$. To test whether this difference reflects the distribution of lithologies, we excluded quartzite and siliciclastic basins that were sampled only to the west of the divide. The east-west difference remains but is significant only at a higher alpha level (0.1). These east-west variations in erosion rates are mirrored by the erosion rates obtained from two of the major rivers draining the Park, the Rappahannock River to the east (13.1 m/My) and the Shenan-

TABLE 5

Erosion rate dependence on aspect

Lithology	East - Average Erosion Rate (m/My)	Number of Samples	West - Average Erosion Rate (m/My)	Number of Samples
Granite	13.2 ± 4.0	7	11.8 ± 4.6	6
Metabasalt*	12.9 ± 7.4	3	7.0 ± 3.8	4
Quartzite**	n/a ± n/a	0	6.9 ± 3.4	8
Siliciclastic	n/a ± n/a	0	10.1 ± 4.2	7
Multilithology	11.0 ± 2.3	3	11.4 ± 6.2	4
Average	13.1 ± 4.4	13	9.0 ± 4.5	29

* Samples SH-02 and SH-18 (temporal replicate) have been averaged.
** Samples SH-36 and SH-41 (temporal replicate) have been averaged.
only non-nested basins used in analysis

doah River to the west (6.6 m/My). The Shenandoah River drainage on the west has lower erosion rates and a higher base-level than the Rappahannock River that drains the eastern margin of the Blue Ridge.

The causes of this significant east-west difference are uncertain and could include rock type, climate forcing, and stream-capture induced base level fall. Weathered metagranites underlie the slopes and lowlands to the east; cosmogenic data show that these rocks erode more rapidly than west-facing quartzites. It is also possible that rock type underlying the trunk streams controls the rate of base level fall and thus the rate at which the tributary basins we sampled erode. To the west, the Harpers Formation, a soft fissile siltstone with intercalcated layers of resistant quartzite, underlies the Page Valley, and the Shenandoah River flows over these clastic rocks rather than the granitic gneisses that underlie the Rappahannock River.

Weather patterns in the Shenandoah region favor more precipitation falling on the eastern side rather than western side of the Blue Ridge (~1500-1800 mm on the east, ~1000-1200 mm on the west; http://www.nationalatlas.gov/printable/images/pdf/precip/pageprecip_va3.pdf, accessed 17 December 2008). Could this be a driver of increased weathering processes and higher erosion rates on the east than on the west? Riebe and others (2001a, 2001b, 2004) suggest that small climate differences like those observed in the Shenandoah region do not greatly influence erosion rates.

The east-west dichotomy in erosion rates could be the result of different landscape history, specifically base-level changes. As suggested earlier, the model of drainage capture for the Appalachian Mountains as proposed by Thompson (1939), Harbor and others (1998, 2005), Pazzaglia and Gardner (1994, 2000), Naeser and others, (2001), and Pazzaglia and others (2006) suggests a means to explain the east/west dichotomy of erosion rates. In this scenario, the Valley and Ridge to Blue Ridge crest relief has remained relatively unchanged since the Miocene. In contrast, relief between the crest and the Piedmont, which lowered significantly after drainage capture, has increased dramatically. Miocene lowering of the Piedmont base-level is supported by thermochronometry data (Spotila and others, 2004) as well as increased sedimentation rates observed in the Baltimore Canyon Trough (Pazzaglia, 1993; Pazzaglia and Gardner, 1994).

The effect of climate and periglacial processes on erosion rates.—While others have noted evidence consistent with the effects of climate change and periglacial processes on landforms in the Blue Ridge region (Clark and Ciolkosz, 1988; Kutzbach and others, 1998; Bard, 2003; Driese and others, 2005; Leigh and Webb, 2006), it is not clear if or

how changing climate regimes affect cosmogenically-determined bedrock and basin-scale erosion rates measured by this and other studies.

Three lines of evidence argue against any significant climatic effect on cosmogenically-determined erosion rates integrated over many millennia: 1) Appalachian Mountain erosion rates calculated from both thermochronometry and sediment accumulation rates (integrated over 10^7 years), match cosmogenically-determined erosion rates integrated over much shorter glacial-interglacial time scales during which significant climate swings (Barron, 1989; Kutzbach and others, 1998; Driese and others, 2005) and periglacial activity occurred (Clark and Ciolkosz, 1988; Barron, 1989; Braun, 1989; Kutzbach and others, 1998; Driese and others, 2005). 2) Riebe and others (2001a, 2004) were unable to detect basin-scale erosion rate differences related to significant differences in temperature and precipitation in drainages underlain by crystalline rocks. 3) Quartz conglomerate and sandstone bedrock surfaces exposed to periglacial activity at Dolly Sods, West Virginia (Hancock and Kirwan, 2007) remained exceptionally stable as determined by large accumulations of ^{10}Be. Dolly Sods average erosion rates (5.7 m/My) are similar to erosion rates we measure in bedrock (6.5 ± 4.3 m/My) cropping out at lower elevations and farther from the glacial margin where periglacial activity was presumably less.

Highland versus lowland erosion rates.—Comparison of erosion rates in the highlands with those of the adjacent lowlands and of the Blue Ridge further to the south suggests the rate and distribution of large scale geomorphic change over time. Despite the presence of easily dissolved carbonate rocks in the Valley and Ridge to the west, the Shenandoah Blue Ridge is lowering (area weighted average ~12.2 m/My) at a rate within the range of prior estimates for the Valley and Ridge, 8 to 30 m/My, (carbonates, White, 1984; White and White, 1991; White, 2000). However, the Shenandoah Blue Ridge is eroding somewhat faster than the low-lying Piedmont province to the east, 4.5 to 8 m/My, (metapelite, metagraywacke, granite, diabase, serpentine, Pavich, 1985); 10 m/My, (Stanford and others, 2002, reconstruction); 9.7 m/My, (micaceous schist and gneiss, Sullivan and others (2006). Together these data suggest that relief between the Blue Ridge and the adjacent piedmont is slowly decreasing, mirroring findings by Sullivan and others (2006) to the south (data in Portenga and Bierman, 2011).

Placing Shenandoah Region Erosion Rates in Context

Cosmogenically determined bedrock and basin-scale erosion rates for the Shenandoah National Park region are in general consistent with those estimated elsewhere in the Appalachian Mountains in a variety of lithologies (Reuter, ms, 2005; Ward and others, 2005; Sullivan and others, 2006; Hancock and Kirwan, 2007; Whitten, ms, 2009; Portenga and others, 2013). Erosion rates for the Shenandoah National Park region with its mixed lithologies (~12 m/My) are indistinguishable from basin-scale erosion rates measured in schist and gneiss (12.5 m/My) for the Blue Ridge just above the Blue Ridge Escarpment (data in Portenga and Bierman, 2011), ~300 km to the south.

The Shenandoah basin-scale erosion rates are similar to those in the Valley and Ridge of the Susquehanna River (Reuter, ms, 2005). The average bedrock erosion rates in and around Shenandoah National Park (6.5 ± 4.3 m/My) are similar to the sandstone on the Appalachian Plateau at Dolly Sods, West Virginia (5.7 m/My) (Hancock and Kirwan, 2007), the average of 29 ridgeline samples in the Blue Ridge Province (6.2 m/My) (Portenga and others, 2013), and that of the granite underlies Panola Mountain in the Georgia Piedmont (7 m/My; Bierman, ms, 1993).

There are some differences between the Shenandoah region and other areas of the southern and central Appalachian Mountains. Average basin-scale rates in the Shenandoah region (~12 m/My) are in general half as fast as those in the Great Smoky Mountains (27 ± 6 m/My; Matmon and others, 2003a; Matmon and others, 2003b).

Despite the similarity of slopes, vegetation and climate in the Great Smoky Mountains and the Shenandoah National Park, this inconsistency points to the fact that the Great Smoky Mountains are anomaly in the realm of Appalachian erosion rates.

Both bedrock (6.5 m/My) and basin-scale erosion rates (~12 m/My) determined in the Shenandoah National Park area are consistent with those measured around the world in diverse, tectonically stable areas, independent of climate (Portenga and Bierman, 2011). Bedrock erosion rates in tectonically stable regions are generally low, despite varying climatic environments, which supports Riebe and others (2001a) conclusion from the Sierra Nevada Mountains that climate only weakly influences erosion rates and further suggests that the east-west dichotomy we observe is not climatically forced. The slow erosion rates measured in Shenandoah and elsewhere in the Appalachian Mountains, suggest that in general this is an area of tectonic stability despite the rugged terrain. These slow erosion rates seem inconsistent with tectonic rejuvenation of the Appalachian Mountains in the Mesozoic as suggested by Poag and Sevon (1989), Pazzaglia (1993), and Pazzaglia and Brandon (1996).

Why does the Blue Ridge of the Shenandoah National Park area look the way it does?—One can consider the Shenandoah cosmogenic data in the context of two long-standing but contrasting qualitative models of landscape behavior, those of Davis and Hack. Examining these models is illustrative, particularly since the lack of significant and pervasive lithologic relationships with basin-scale erosion rates appears to contradict the long-standing observation that structure and lithology control the large-scale geomorphology of the Shenandoah region.

Davis' *Geographic Cycle* (1899), developed from observations in the Susquehanna River Basin and the Appalachian Mountains, describes how topography changes over time. Davis' model is based on the *peneplain concept* where in an unperturbed landscape, topography will diminish over time, until only a flat, low relief peneplain exists. The Davis model is consistent with a positive relationship between slope and erosion rate, such as that we observed in Shenandoah National Park with high-slope basins eroding more rapidly than low-slope basins.

Alternatively, Hack's (1960) model of *dynamic equilibrium* describes landscape morphology that is adjusted to the erosional resistance of the underlying rock over the long-term. In Hack's schema, differences in erosional resistance or rock strength are compensated for by slope. Less resistant lithologies have low slopes, and more resistant lithologies have steeper slopes; yet, all erode at similar rates. In Hack's view, erosion rates are similar across the landscape with slope being adjusted to rock strength. Analysis of the Shenandoah data set as a whole and of individual lithologies indicates a positive erosion rate/slope relationship. The Shenandoah dataset suggests that slope, lithology, and aspect are correlated with erosion rates, inferring non-uniform erosion across the landscape and therefore not supporting Hack's model of *dynamic equilibrium* at the drainage basin scale.

In a modern adaptation of Hack's theme, cosmogenic data from Riebe and others (2000) for very small basins in the Sierra Nevada Mountains, suggest that slope and erosion rate co-vary only when base-level has lowered and the landscape upstream has not yet adjusted. If the supposition of Riebe and others (2000) is correct, the base-level to which the Shenandoah regions' streams are graded has fallen consistent with suggestion of Miocene trunk stream capture. Stream profiles in the Shenandoah region did not reveal distinct features associated with stream adjustment such as knickpoints, but this does not necessarily rule out the possibility that the streams and basins are in a period of adjustment. Broader application of this line of reasoning suggests that base-level fall and consequent landscape adjustment is still occurring in the Susquehanna River Basin, the Great Smoky Mountains, and the Blue Ridge Escarpment areas.

If quartzite is the most resistant rock in this region, why isn't it holding up the highlands? To answer this question it is necessary to examine the geologic controls operating within the Park. Quartzites underlie Massanutten Mountain (west of Blue Ridge) and low hills along the west flank of the Blue Ridge. These low hills are in the footwall of Late Paleozoic thrust faults, which decapitated the folded quartzite strata, that is, they never cropped out at a much higher elevation. North of the Stanley Fault at Thornton Gap (Bailey and others, 2006), flat-lying quartzite does underlie a highland area. Reconstructions of cross-sections show that the current morphology of the Blue Ridge is a function of the erosion level on faulted and folded strata that plunge to the northeast. Structurally higher areas have been eroded down to Mesoproterozoic granite (Bailey and others, 2006). Locally, the near flat-lying metabasalt overlies the granite and caps the highlands along the ridgeline, and at lower elevations, the flat-lying quartzite overlies the metabasalt. Hack (1982) suggested that the lower altitude of the Chilhowee Group rocks is indicative of less resistance than the metabasalt (Catoctin Formation) and granite (Pedlar Formation). Given the similar erosion rates for different lithologies measured in this study, it is more likely that the altitude of the Chilhowee Group is due to geologic controls, rather than any difference in erosional resistance.

All things being constant, the cap rocks will continue to erode, exposing the underlying strata as the landscape is lowered (Bailey and others, 2006). It appears that structure in part controls landscape morphology and erosion has yet to exert control on a scale sufficient to alter these structurally controlled large-scale geomorphic patterns. Shenandoah has not yet reached a state of Hackian equilibrium whereas continued isostatic response to denudation, albeit slow, prevents Davisian peneplanation. In summary, it appears that structure does matter but that neither qualitative model, Davis or Hack, explains well the overall geomorphic history of Shenandoah National Park. Rather, the appearance and erosional behavior of the park landscape we see today is the result of long-term trunk stream history superimposed on the underlying geology.

CONCLUSION

The metamorphic rocks of the Shenandoah National Park region do not fit into the simple landscape model of ridge-capping resistant rocks that has been applied to other areas of the Appalachian Mountains (Matmon and others, 2003a; Matmon and others, 2003b; Reuter, ms, 2005). In the Park highlands, metabasalt and metagranites, rather than the more erosion-resistant quartzite, form the ridgeline. The correlation between erosion rates and slope/aspect/lithology is inconsistent with Hack's (1960) model of *dynamic equilibrium* where landscape morphology is adjusted to the erosional resistance of the underlying rock over the long-term.

The consistency of the cosmogenic erosion data with long term denudation rates inferred from other techniques suggests that glacial-interglacial climate variations do not have a significant impact on time-integrated erosion rates. The landscape of the Blue Ridge Province is a product of slow erosion, with multi-millennial erosion rates averaging ~12 m/My, similar to post-orogenic denudation rates integrated over time periods several orders of magnitude longer. This steady erosion over time suggests that the region's landscape may well have remained grossly similar for millions of years. Slow denudation of ancient rocks is most likely driving gradual but continual isostatic uplift that maintains self-similar topography (Pavich, 1985) controlled by rock competence and structure.

Cosmogenic analysis of bedrock and sediment from the Shenandoah Park area as well as other sites in the southern Appalachians allows us to speculate about why some parts of the Appalachian Mountains erode slowly and some more rapidly. Overall, it appears that steep drainage basins erode more rapidly than gently sloped basins.

Climate and lithology appear to play less important roles in determining basin-scale rates of erosion at least for quartz-bearing rocks. There are significant hints that past geomorphic history is important as exemplified by the east-west dichotomy in erosion rates we determined in the Shenandoah area. Data are conflicting in regards to the evolution of relief over time. Analyses that have been made of exposed bedrock along ridgelines suggests that such rock is eroding either more slowly than adjacent drainage basins (Susquehanna - Reuter, ms, 2005; this study) or at similar rates (Great Smoky Mountains - Matmon and others, 2003a, 2003b) proving a mechanism for growing relief at the scale of individual ridgelines. However, considering relief on a landscape or physiographic province scale by comparing erosion rates of the highlands versus the lowlands, suggests that relief of the range as a whole is either steady or at most slowly decreasing over multi-millennial timescales. This finding supports a broad Hackian view of the landscape, the idea that there is a dynamic steady state driven by isostatic compensation of erosion at very slow rates.

ACKNOWLEDGMENTS

This project was supported by funds from the U.S. Geological Survey (04ERAG0064-0001) and National Science Foundation grant EAR-310208 to P. R. Bierman. We thank D. Fabel at Glasgow University for providing space for sample processing in the Glasgow University-SUERC Cosmogenic Nuclide Laboratory at SUERC, R. Finkel and the Center for Accelerator Mass Spectrometry at the Lawrence Livermore National Laboratory for analyzing the initial samples, J. Aleong for assistance with statistical analysis and J. Spotila, B. Morgan, and D. Doctor for constructive reviews.

References

Badger, R. L., and Sinha, A. K., 1988, Age and Sr isotopic signature of the Catoctin volcanic province: Implications for subcrustal mantle evolution: Geology, v. 16, n. 8, p. 692–695, http://dx.doi.org/10.1130/0091-7613(1988)016<0692:AASISO>2.3.CO;2

Bailey, C. M., Southworth, S., and Tollo, R. P., 2006, Tectonic history of the Blue Ridge, north-central Virginia, *in* Pazzaglia, F. J., editor, Excursions in Geology and History: Field Trips in the Middle Atlantic States: Boulder, The Geological Society of America, p. 22.

Balco, G., Stone, J. O., Lifton, N. A., and Dunai, T. J., 2008, A complete and easily accessible means of calculating surface exposure ages or erosion rates from ^{10}Be and ^{26}Al measurements: Quaternary Geochronology, v. 3, n. 3, p. 174–195, http://dx.doi.org/10.1016/j.quageo.2007.12.001

Bard, E., 2003, North-Atlantic sea surface temperature reconstruction: IGBP PAGES/World Data Center for Paleoclimatology Data Contribution Series, v. 26.

Barron, E. J., 1989, Climate variations and the Appalachians from the Late Paleozoic to the present: Results from Model Simulations: Geomorphology, v. 2, n. 1–3, p. 99–118, http://dx.doi.org/10.1016/0169-555X(89)90008-1

Belmont, P., Pazzaglia, F. J., and Gosse, J., 2006, Using the 10-Be grain size dependency in alluvial sediments to investigate hillslope and channel processes: American Geophysical Union, Fall Meeting 2006, abstract# H21H-06.

Bierman, P., and Nichols, K. K., 2004, Rock to sediment - Slope to sea with ^{10}Be - Rates of landscape change: Annual Review of Earth and Planetary Sciences, v. 32, p. 215–255, http://dx.doi.org/10.1146/annurev.earth.32.101802.120539

Bierman, P. R., ms, 1993, *In situ* produced cosmogenic isotopes and the evolution of granitic landforms: Seattle, Washington, University of Washington, Ph. D. Thesis, p. 289.

——— 1994, Using *in situ* produced cosmogenic isotopes to estimate rates of landscape evolution: A review from the geomorphic perspective: Journal of Geophysical Research, Solid Earth, v. 99, n. B7, p. 13885–13896, http://dx.doi.org/10.1029/94JB00459

Bierman, P. R., and Caffee, M. W., 2001, Slow rates of rock surface erosion and sediment production across the Namib Desert and escarpment, Southern Africa: American Journal of Science, v. 301, n. 4–5, p. 326–358, http://dx.doi.org/10.2475/ajs.301.4-5.326

Bierman, P. R., and Steig, E., 1996, Estimating rates of denudation and sediment transport using cosmogenic isotope abundances in sediment: Earth Surface Processes and Landforms, v. 21, n. 2, p. 125–139, http://dx.doi.org/10.1002/(SICI)1096-9837(199602)21:2<125::AID-ESP511>3.0.CO;2-8

Bierman, P .R., Albrecht, A., Bothner, M., Brown, E., Bullen, T., Gray, L., and Turpin, L., 1998, Weathering, erosion and sedimentation, *in* Kendall, C., and McDonnell, J. J., editors, Isotope Tracers in Catchment Hydrology, chapter 23: Amsterdam, Elsevier, p. 647–678.

Bierman, P. R., Caffee, M. W., Davis, P. T., Marsella, K., Pavich, M., Colgan, P., Mickelson, D., and Larsen, J., 2002, Rates and timing of Earth surface processes from *in situ*-produced cosmogenic Be-10, *in* Grew,

E. S., editor, Beryllium; mineralogy, petrology, and geochemistry: Reviews in Mineralogy and Geochemistry, v. 50, p. 147–205, http://dx.doi.org/10.2138/rmg.2002.50.4
Bishop, P., 2007, Long-term landscape evolution: linking tectonics and surface processes: Earth Surface Processes and Landforms, v. 32, n. 3, p. 329–365, http://dx.doi.org/10.1002/esp.1493
Blackmer, G. C., Omar, G. I., and Gold, D. P., 1994, Post-Alleghanian unroofing history of the Appalachian Basin, Pennsylvania, from apatite fission track analysis and thermal models: Tectonics, v. 13, n. 5, p. 1259–1276, http://dx.doi.org/10.1029/94TC01507
Boettcher, S. S., and Milliken, K. L., 1994, Mesozoic-Cenozoic unroofing of the southern Appalachian Basin: Apatite fission track evidence from Middle Pennsylvanian sandstones: The Journal of Geology, v. 102, n. 6, p. 655–663, http://dx.doi.org/10.1086/629710
Braun, D. D., 1989, Glacial and periglacial erosion of the Appalachians: Geomorphology, v. 2, n. 1–3, p. 233–256, http://dx.doi.org/10.1016/0169-555X(89)90014-7
Brown, E. T., Stallard, R. F., Larsen, M. C., Raisbeck, G. M., and Yiou, F., 1995, Denudation rates determined from the accumulation of *in situ*-produced ^{10}Be in the Luquillo Experimental Forest, Puerto Rico: Earth and Planetary Science Letters, v. 129, n. 1–4, p. 193–202, http://dx.doi.org/10.1016/0012-821X(94)00249-X
Child, D., Elliott, G., Mifsud, C., Smith, A. M., and Fink, D., 2000, Sample processing for earth science studies at ANTARES: Nuclear Instruments and Methods in Physics Research, B, Beam Interactions with Materials and Atoms, v. 172, n. 1–4, p. 856–860, http://dx.doi.org/10.1016/S0168-583X(00)00198-1
Chirico, P., and Tanner, S., 2004, Shaded relief image map of topogrid derived 10 meter resolution digital elevation model of the Shenandoah National Park and surrounding region, Virginia, U.S: United States Geological Survey Open-File Report 04-1321.
Clapp, E. M., Bierman, P. R., and Caffee, M., 1997, Rates of erosion determined using in situ produced cosmogenic isotopes in a small arroyo basin, northwestern New Mexico: Geological Society of America, 1997 annual meeting Abstracts with Programs , v. 29, p. 371–372.
——— 1998, Estimating long-term erosion rates in a hyper-arid region using *in situ* produced cosmogenic 10-Be and 26-Al in sediment and bedrock: Geological Society of America, 1998 annual meeting Abstracts with Programs, v. 30, p. 361.
——— 2002, Using ^{10}Be and ^{26}Al to determine sediment generation rates and identify sediment source areas in an arid region drainage basin: Geomorphology, v. 45, n. 1–2, p. 89–104, http://dx.doi.org/10.1016/S0169-555X(01)00191-X
Clapp, E. M., Bierman, P. R., Nichols, K. K., Pavich, M., and Caffee, M., 2001, Rates of sediment supply to arroyos from upland erosion determined using *in situ* produced cosmogenic ^{10}Be and ^{26}Al: Quaternary Research, v. 55, n. 2, p. 235–245, http://dx.doi.org 10.1006/qres.2000.2211
Clark, G. M., and Ciolkosz, E. J., 1988, Periglacial geomorphology of the Appalachian Highlands and Interior Highlands south of the glacial border: a review: Geomorphology, v. 1, n. 3, p. 191–200, http://dx.doi.org/10.1016/0169-555X(88)90014-1
Davis, W. M., 1899, The geographical cycle: Geographical Journal, v. 14, n. 5, p. 481–504, http://dx.doi.org/10.2307/1774538
Desilets, D., and Zreda, M., 2000, Scaling production rates of terrestrial cosmogenic nuclides for altitude and geomagnetic effects: Geological Society of America Abstracts with Programs, v. 31, p. A-400.
Driese, S. G., Li, Z.-H., and Horn, S. P., 2005, Late Pleistocene and Holocene climate and geomorphic histories as interpreted from a 23,000 ^{14}C yr B.P. paleosol and floodplain soils, southeastern West Virginia, USA: Quaternary Research, v. 63, n. 2, p. 136–149, http://dx.doi.org/10.1016/j.yqres.2004.10.005
Dunai, T. J., 2000, Scaling factors for production rates of *in situ* produced cosmogenic nuclides: a critical reevaluation: Earth and Planetary Science Letters, v. 176, n. 1, p. 157–169, http://dx.doi.org/10.1016/S0012-821X(99)00310-6
Eaton, L. S., Morgan, B. A., Kochel, C., R., and Howard, A. D., 2003a, Quaternary deposits and landscape evolution of the central Blue Ridge of Virginia: Geomorphology, v. 56, n. 1–2, p. 139–154, http://dx.doi.org/10.1016/S0169-555X(03)00075-8
——— 2003b, Role of debris flows in long-term landscape denudation in the central Appalachians of Virginia: Geology, v. 31, n. 4, p. 339–342, http://dx.doi.org/10.1130/0091-7613(2003)031<0339:RODFIL>2.0.CO;2
Galloway, R. W., 1961, Periglacial Phenomena in Scotland: Geografiska Annaler, v. 43, n. 3–4, p. 348–353, http://dx.doi.org/10.2307/520131
Gathright, T. M., II, 1976, Geology of the Shenandoah National Park, Virginia: Virginia Division of Mineral Resources Bulletin, v. 86, p. 93.
Gosse, J. C., and Phillips, F. M., 2001, Terrestrial *in situ* cosmogenic nuclides: theory and application: Quaternary Science Reviews, v. 20, n. 14, p. 1475–1560, http://dx.doi.org/10.1016/S0277-3791(00)00171-2
Goudie, A., 1995, The Changing Earth: Rates of Geomorphological Processes: Oxford, Blackwell, 352 p.
Granger, D. E., Kirchner, J. W., and Finkel, R., 1996, Spatially averaged long-term erosion rates measured from *in situ*-produced cosmogenic nuclides in alluvial sediments: The Journal of Geology, v. 104, n. 3, p. 249–257, http://dx.doi.org/10.1086/629823
——— 1997, Quaternary downcutting rate of the New River, Virginia, measured from differential decay of cosmogenic ^{26}Al and ^{10}Be in cave-deposited alluvium: Geology, v. 25, n. 2, p. 107–110, http://dx.doi.org/10.1130/0091-7613(1997)025<0107:QDROTN>2.3.CO;2
Hack, J. T., 1960, Interpretation of erosional topography in humid temperate regions: American Journal of Science, v. 258A, p. 80–97.
——— 1965, Geomorphology of the Shenandoah Valley, Virginia and West Virginia, and origin of the residual ore deposits: US Geological Survey Professional Paper, v. 484, p. 84.

——— 1982, Physiographic divisions and differential uplift in the Piedmont and Blue Ridge: US Geological Survey Professional Paper, v. 1265, p. 49.
Hancock, G., and Kirwan, M., 2007, Summit erosion rates deduced from ^{10}Be: Implications for relief production in the central Appalachians: Geology, v. 35, n. 1, p. 89–92, http://dx.doi.org/10.1130/G23147A.1
Harbor, D., Bacastow, A., Heath, A., and Rogers, J., 1998, Cenozoic landscape evolution in the southern Shenandoah Valley, Virginia: Lexington, Kentucky, 11th Keck Geology Consortium Undergraduate Research Symposia, p. 222–225.
——— 2005, Capturing variable knickpoint retreat in the central Appalachians, USA: Geografia Fisica e Dinamica Quaternaria, v. 28, p. 23–26.
Harris, S. E., and Mix, A. C., 2002, Climate and tectonic influences on continental erosion of tropical South America, 0-13 Ma: Geology (Boulder), v. 30, p. 447–450.
Heimsath, A. M., Chappell, J., Dietrich, W. E., Nishiizumi, K., and Finkel, R. C., 2000, Soil production on a retreating escarpment in southeastern Australia: Geology, v. 28, n. 9, p. 787–790, http://dx.doi.org/10.1130/0091-7613(2000)28<787:SPOARE>2.0.CO;2
Heimsath, A. M., Dietrich, W. E., Nishiizumi, K., and Finkel, R. C., 1999, Cosmogenic nuclides, topography, and the spatial variation of soil depth: Geomorphology, v. 27, n. 1–2, p. 151–172, http://dx.doi.org/10.1016/S0169-555X(98)00095-6
——— 2001, Stochastic processes of soil production and transport; erosion rates, topographic variation and cosmogenic nuclides in the Oregon Coast Range: Earth Surface Processes and Landforms, v. 26, n. 5, p. 531–552, http://dx.doi.org/10.1002/esp.209
Hills, R. C., 1969, Comparative weathering of granite and quartzite in a periglacial environment: Geografiska Annaler Series A, Physical Geography, v. 51, p. 46–47.
King, P. B., 1950, Geology of the Elkton area, Virginia: US Geological Survey Professional Paper, v. 230, p. 82.
Kiver, E. P., and Harris, D. V., 1999, Geology of U.S. Parklands: New York, John Wiley, 912 pages.
Kochel, R. C., and Johnson, R. A., 1984, Geomorphology and sedimentology of humid-temperate alluvial fans, central Virginia: Sedimentology of gravels and conglomerates: Canadian Society of Petroleum Geologists Memoir, v. 10, p. 109–122.
Kohl, C. P., and Nishiizumi, K., 1992, Chemical isolation of quartz for measurement of *in-situ*-produced cosmogenic nuclides: Geochimica et Cosmochimica Acta, v. 56, n. 9, p. 3583–3587, http://dx.doi.org/10.1016/0016-7037(92)90401-4
Kutzbach, J., Gallimore, R., Harrison, S., Behling, P., Selin, R., and Laarif, F., 1998, Climate and biome simulations for the past 21,000 years: Quaternary Science Reviews, v. 17, n. 6–7, p. 473–506, http://dx.doi.org/10.1016/S0277-3791(98)00009-2
Lal, D., 1988, *In situ*-produced cosmogenic isotopes in terrestrial rocks: Annual Review of Earth and Planetary Science, v. 16, p. 355–388, http://dx.doi.org/10.1146/annurev.ea.16.050188.002035
——— 1991, Cosmic ray labeling of erosion surfaces; *in situ* nuclide production rates and erosion models: Earth and Planetary Science Letters, v. 104, n. 2–4, p. 424–439, http://dx.doi.org/10.1016/0012-821X(91)90220-C
——— 1998, Cosmic ray produced isotopes in terrestrial systems: Journal of Earth System Science, v. 107, n. 4, p. 241–249, http://dx.doi.org/10.1007/BF02841592
Lal, D., and Peters, B., 1967, Cosmic ray produced radioactivity on the earth, *in* Sitte, K., editor, Handbuch der Physik: New York, Springer-Verlag, Encyclopedia of Physics, v. 9/46/2, p. 551–612, http://dx.doi.org/10.1007/978-3-642-46079-1_7
Leigh, D. S., and Webb, P. A., 2006, Holocene erosion, sedimentation, and stratigraphy at Raven Fork, Southern Blue Ridge Mountains, USA: Geomorphology, v. 78, n. 1–2, p. 161–177, http://dx.doi.org/10.1016/j.geomorph.2006.01.023
Lifton, N. A., 2000, A robust scaling model for *in situ* cosmogenic nuclide production rates: Geological Society of America Abstracts with Programs, v. 31, A-400.
Litwin, R. J., Morgan, B., Eaton, S., Wieczorek, G., and Smoot, J. P., 2001, Proxy climate evidence from Late Pleistocene Deposits in the Blue Ridge of Virginia: US Geological Survey Open File Report, p. 01-406.
Matmon, A., Bierman, P. R., Larsen, J., Southworth, S., Pavich, M., and Caffee, M., 2003a, Temporally and spatially uniform rates of erosion in the southern Appalachian Great Smoky Mountains: Geology, v. 31, n. 2, p. 155–158, http://dx.doi.org/10.1130/0091-7613(2003)031<0155:TASURO>2.0.CO;2
Matmon, A. S., Bierman, P. R., Larsen, J., Southworth, S., Pavich, M., Finkel, R., and Caffee, M., 2003b, Erosion of an ancient mountain range, the Great Smoky Mountains, North Carolina and Tennessee: American Journal of Science, v. 303, n. 9, p. 817–855, http://dx.doi.org/10.2475/ajs.303.9.817
Merschat, C. E., 1997, Geology of Yancy County: Raleigh, North Carolina Geological Survey, Division of Land Resources, p. 22.
Miller, S. R., Sak, P. B., Kirby, E., and Bierman, P. R., 2013, Neogene rejuvenation of central Appalachian topography: Evidence for differential rock uplift from stream profiles and erosion rates: Earth and Planetary Science Letters, v. 369–370, p. 1–12, http://dx.doi.org/10.1016/j.epsl.2013.04.007
Morgan, B. A., Wieczorek, G. F., and Campbell, R. H., 1999, Map of rainfall, debris flows, and flood effects of the June 27, 1995, storm in Madison County, Virginia: United States Geological Survey Geologic Investigation Series Map I-2623A, 1:24,000.
Morgan, B. A., Eaton, L. S., and Wieczorek, G. F., 2004, Pleistocene and Holocene colluvial fans and terraces in Shenandoah National Park, Virginia: U.S. Geological Survey, Open-File Report 03-410, 25 p.
Naeser, C. W., Naeser, N. D., Kunk, M. J., Morgan Iii, B. A., Schultz, A. P., Southworth, C. S., and Weems, R. E., 2001, Paleozoic through Cenozoic uplift, erosion, stream capture, and deposition history in the Valley and Ridge, Blue Ridge, Piedmont, and Coastal Plain provinces of Tennessee, North Carolina, Virginia, Maryland, and District of Columbia: Geological Society of America Annual Meeting, abstract 133-0.

Naeser, N. D., Naeser, C. W., Southworth, C. S., Morgan, B. A., and Schultz, A. P., 2004, Paleozoic to recent tectonic and denudation history of rocks in the Blue Ridge province, central and southern Appalachians - evidence from fission-track thermochronology: Geological Society of America Abstracts with Programs, p. 114.

Naeser, C. W., Naeser, N. D., and Southworth, C. S., 2005, Tracking Across the southern Appalachians *in* Blue Ridge Geology Geotraverse East of the Great Smoky Mountains National Park, Western North Carolina: North Carolina Geological Survey, Carolina Geological Society Annual Fieldtrip Guidebook, p. 67–72

——— 2006a, Tracking Across the Southern Appalachians: Eastern Tennessee and Western Carolinas: Geological Society of America Abstracts with Programs, p. 67.

Naeser, N. D., Naeser, C. W., Newell, W. L., Southworth, S., Weems, R. E., and Edwards, L. E., 2006b, Provenance studies in the Atlantic Coastal Plain: What fission-track ages of detrital zircons can tell us about the erosion history of the Appalachians: Geological Society of America Abstracts with Programs, 2006 Philadelphia Annual Meeting, p. 503.

Nishiizumi, K., Lal, D., Klein, J., Middleton, R., and Arnold, J. R., 1986, Production of ^{10}Be and ^{26}Al by cosmic rays in terrestrial quartz *in situ* and implications for erosion rates: Nature, v. 319, p. 134–136, http://dx.doi.org/10.1038/319134a0

Nishiizumi, K., Imamura, M., Caffee, M. W., Southon, J. R., Finkel, R. C., and McAninch, J., 2007, Absolute calibration of ^{10}Be AMS standards: Nuclear Instruments and Methods in Physics Research Section B: Beam Interactions with Materials and Atoms, v. 258, n. 2, p. 403–413, http://dx.doi.org/10.1016/j.nimb.2007.01.297

Pavich, M., 1985, Appalachian piedmont morphogenesis: weathering, erosion, and Cenozoic uplift, *in* Morisawa, M., and Hack, J., editors, Tectonic Geomorphology: Binghampton, New York, State University of New York, Proceedings of the 15th Annual Geomorphology Symposium Series, p. 299–319.

——— 1990, Characteristics, origin, and residence time of saprolite and soil of the Piedmont upland, Virginia, U.S.A., and model testing using cosmogenic ^{10}Be, *in* Noack, Y., Nahon, D., Alexander, R., Allegre, C. J., Crerar, D. A., Hofmann, A. W., Kushiro, I., Lasaga, A. C., and Taylor, H. P., editors, Geochemistry of the Earth's Surface and of Mineral Formation, 2nd International Symposium, Aix en Provence, France: Chemical Geology, v. 84, n. 1–4, p. 15–16, http://dx.doi.org/10.1016/0009-2541(90)90148-Z

Pazzaglia, F. J., 1993, Stratigraphy, petrography, and correlation of late Cenozoic middle Atlantic Coastal Plain deposits: Implications for late-stage passive-margin geologic evolution: Geological Society of America Bulletin, v. 105, p. 1617–1634.

Pazzaglia, F. J., and Brandon, M. T., 1996, Macrogeomorphic evolution of the post-Triassic Appalachian mountains determined by deconvolution of the offshore basin sedimentary record: Basin Research, v. 8, p. 255–278.

Pazzaglia, F. J., and Gardner, T. W., 1994, Late Cenozoic flexural deformation of the middle U. S. Atlantic passive margin: Journal of Geophysical Research-Solid Earth, n. B6, v. 99, p. 12,143–12,157, http://dx.doi.org/10.1029/93JB03130

——— 2000, Late Cenozoic landscape evolution of the US Atlantic passive margin-Insights into a North American Great Escarpment, *in* Summerfield, M., editor, Geomorphology and Global Tectonics: New York, John Wiley, p. 283–302.

Pazzaglia, F. J., Braun, D. D., Pavich, M., Bierman, P., Potter Jr., N., Merritts, D., Walter, R., and Germanoski, D., 2006, Rivers, glaciers, landscape evolution, and active tectonics of the central Appalachians, Pennsylvania and Maryland, *in* Pazzaglia, F. J., editor, Excursions in Geology and History: Field Trips in the Middle Atlantic States: Boulder, Colorado, The Geological Society of America, p. 247.

Pierce, K. L., 1965, Geomorphic significance of Cretaceous deposits in the Great Valley of southern Pennsylvania: US Geological Survey, Professional Paper 525-C, p. C152–C156.

Poag, C. W., and Sevon, W. D., 1989, A record of Appalachian denudation in postrift Mesozoic and Cenozoic sedimentary deposits of the U.S. middle Atlantic continental margin: Geomorphology, v. 2, n. 1–3, p. 119–157, http://dx.doi.org/10.1016/0169-555X(89)90009-3

Portenga, E. W., and Bierman, P. R., 2011, Understanding Earth's eroding surface with ^{10}Be: GSA Today, v. 21, n. 8, p. 4–10, http://dx.doi.org/10.1130/G111A.1

Portenga, E.W., Bierman, P. R., Rizzo, D. M., and Rood, D. H., 2013, Low rates of bedrock outcrop erosion in the central Appalachian Mountains inferred from *in situ* ^{10}Be: Geological Society of America Bulletin. v. 125, n. 1–2, p. 201–215, http://dx.doi.org/10.1130/B30559.1

Reed Jr., J. C., 1955, Catoctin Formation near Luray: Virginia: Geological Society of America Bulletin, v. 66, n. 7, p. 871–896, http://dx.doi.org/10.1130/0016-7606(1955)66[871:CFNLV]2.0.CO;2

Reed, J. S., Spotila, J. A., Eriksson, K. A., and Bodnar, R. J., 2005, Burial and exhumation history of Pennsylvanian strata, central Appalachian basin: an integrated study: Basin Research, v. 17, n. 2, p. 259–268, http://dx.doi.org/10.1111/j.1365-2117.2005.00265.x

Reiners, P. W., and Brandon, M. T., 2006, Using thermochronology to understand orogenic erosion: Annual Review of Earth and Planetary Sciences, v. 34, p. 419–466, http://dx.doi.org/10.1146/annurev.earth.34.031405.125202

Reuter, J. M., ms, 2005, Erosion rates and patterns inferred from cosmogenic ^{10}Be in the Susquehanna River Basin: Burlington, Vermont, University of Vermont, Masters Thesis, 172 p.

Riebe, C. S., Kirchner, J. W., Granger, D. E., and Finkel, R. C., 2000, Erosional equilibrium and disequilibrium in the Sierra Nevada, inferred from cosmogenic ^{26}Al and ^{10}Be in alluvial sediment: Geology, v. 28, n. 9, p. 803–806, http://dx.doi.org/10.1130/0091-7613(2000)28<803:EEADIT>2.0.CO;2

——— 2001a, Minimal climatic control on erosion rates in the Sierra Nevada, California: Geology, v. 29, n. 5, p. 447–450, http://dx.doi.org/10.1130/0091-7613(2001)029<0447:MCCOER>2.0.CO;2

——— 2001b, Strong tectonic and weak climatic control of long-term chemical weathering rates: Geology, v. 29, n. 6, p. 511–514, http://dx.doi.org/10.1130/0091-7613(2001)029<0511:STAWCC>2.0.CO;2
Riebe, C. S., Kirchner, J. W., and Finkel, R. C., 2003, Long-term rates of chemical weathering and physical erosion from cosmogenic nuclides and geochemical mass balance: Geochimica et Cosmochimica Acta, v. 67, n. 22, p. 4411–4427, http://dx.doi.org/10.1016/S0016-7037(03)00382-X
——— 2004, Erosional and climatic effects on long-term chemical weathering rates in granitic landscapes spanning diverse climate regimes: Earth and Planetary Science Letters, v. 224, n. 3–4, p. 547–562, http://dx.doi.org/10.1016/j.epsl.2004.05.019
Roden, M. K., 1991, Apatite fission-track thermochronology of the southern Appalachian Basin: Maryland, West Virginia, and Virginia: The Journal of Geology, v. 99, n. 1, p. 41–53, http://dx.doi.org/10.1086/629472
Rodgers, J., 1970, The Tectonics of the Appalachians: New York, Wiley-Interscience, 271 p.
Smoot, J. P., 2004, Sedimentary fabrics of stratified slope deposits at a site near Hoover's Camp, Shenandoah National Park, Virginia: US Geological Survey Open-File Report 2004- 1059, 49 p.
Southworth, S., Drake Jr., A. A., Brezinski, D. K., Wintsch, R. P., Kunk, M. J., Aleinikoff, J. N., Naeser, C. W., and Naeser, N. D., 2006, Central Appalachian Piedmont and Blue Ridge tectonic transect, Potomac River corridor: Excursions in Geology and History: Field Trips in the Middle Atlantic States: Geological Society of America Field Guide 8, p. 135–167, http://dx.doi.org/10.1130/2006.fld008(08)
Southworth, S., Aleinikoff, J. N., Bailey, C. M., Burton, W. C., Crider, E. A., Hackley, P. C., Smoot, J. P., and Tollo, R. P., 2009, Geologic map of the Shenandoah National Park region Virginia: U.S. Geological Survey Open-File Report 2009–1153, 96 p., 1 plate, scale 1:100,000.
Spotila, J. A., Bank, G. C., Reiners, P. W., Naeser, C. W., Naeser, N. D., and Henika, B. S., 2004, Origin of the Blue Ridge escarpment along the passive margin of Eastern North America: Basin Research, v. 16, n. 1, p. 41–63, http://dx.doi.org/10.1111/j.1365-2117.2003.00219.x
Stanford, S. D., Ashley, G. M., Russell, E. W. B., and Brenner, G. J., 2002, Rates and patterns of late Cenozoic denudation in the northernmost Atlantic Coastal Plain and Piedmont: Bulletin of the Geological Society of America, v. 114, n. 11, p. 1422–1437, http://dx.doi.org/10.1130/0016-7606(2002)114<1422:RAPOLC>2.0.CO;2
Stose, G. W., Miser, H. D., Katz, F. J., and Hewett, D. F., 1919, Manganese deposits of the west foot of the Blue Ridge, Virginia: Virginia Geological Survey Bulletin v. 17, 166 p.
Sullivan, C. L., Bierman, P., Pavich, M., Larsen, J., and Finkel, R., 2006, Cosmogenically derived erosion rates for the Blue Ridge Escarpment, Southern Appalachian Mountains: Geological Society of America Abstracts with Programs, 2006 Philadelphia Annual Meeting, p. 279.
Thompson, H. D., 1939, Drainage evolution in the Southern Appalachians: Geological Society of America Bulletin, v. 50, n. 8, p. 1323–1356, http://dx.doi.org/10.1130/GSAB-50-1323
Tollo, R. P., Bailey, C. M., Borduas, E. A., and Aleinikoff, J. N., 2004, 2. Mesoproterozoic Geology of the Blue Ridge Province in North-Central Virginia: Petrologic and Structural Perspectives on Grenvillian Orogenesis and Paleozoic Tectonic Processes, *in* Southworth, S., and Burton, W., editors, Geology of the National Capital Region - Field Trip Guide Book: Tysons, U.S. Geological Survey Circular 1264, p. 17–75.
Tollo, R. P., Aleinikoff, J. N., Borduas, E. A., Dickin, A. P., McNutt, R. H., and Fanning, C. M., 2006, Grenvillian magmatism in the northern Virginia Blue Ridge: Petrologic implications of episodic granitic magma production and the significance of postorogenic A-type charnockite: Precambrian Research, v. 151, n. 3–4, p. 224–264, http://dx.doi.org/10.1016/j.precamres.2006.08.010
Trodick, C., Bierman, P. R., Pavich, M., Reusser, L., Portenga, E., and Rood, D., 2010, Basin scale erosion rates from the Potomac River Basin using *in situ* and meteoric ^{10}Be: Geological Society of America Abstracts with Programs, v. 42, n. 5, p. 33.
von Blanckenburg, F., 2005, The control mechanisms of erosion and weathering at basin scale from cosmogenic nuclides in river sediment: Earth and Planetary Science Letters, v. 237, n. 3–4, p. 462–479, http://dx.doi.org/10.1016/j.epsl.2005.06.030
von Blanckenburg, F., Hewawasam, T., and Kubik, P. W., 2004, Cosmogenic nuclide evidence for low weathering and denudation in the wet, tropical highlands of Sri Lanka: Journal of Geophysical Research-Earth Surface, v. 109, n. F3, http://dx.doi.org/10.1029/2003JF000049
Ward, D. J., Spotila, J. A., Hancock, G. S., and Galbraith, J. M., 2005, New constraints on the late Cenozoic incision history of the New River, Virginia: Geomorphology, v. 72, n. 1–4, p. 54–72, http://dx.doi.org/10.1016/j.geomorph.2005.05.002
Washburn, A. L., 1973, Periglacial processes and environments: London, Edward Arnold, 320 p.
——— 1980, Geocryology: a survey of periglacial processes and environments: New York, Wiley, 406 p.
White, W. B., 1984, Rate processes: chemical kinetics and karst landform development: Groundwater as a Geomorphic Agent, p. 227–248.
——— 2000, Dissolution of limestone from field observations, *in* Klimchouk, A. B., Ford, D. C., Palmer, A. N., and Dreybrodt, W., editors, Speleogenesis: Evolution of Karst Aquifers: Huntsville, Alabama, National Speleological Society, 527 p.
White, W. B., and White, E. L., 1991, Karst erosion surfaces in the Appalachian highlands: Appalachian Karst, *in* Kastning E., and Kastning, K. M., editors, Proceedings of the Appalachian Karst Symposium: Huntsville, Alabama, National Speleological Society, p. 1–10.
Whittecar, G. R., 1992, Alluvial fans and boulder streams of the Blue Ridge Mountains, west-central Virginia: Norfolk, Virginia, Old Dominion University, Southeastern Friends of the Pleistocene, 1992 Field Trip Guidebook, 128 p.
Whitten, J., ms, 2009, Bare bedrock erosion rates in the central Appalachians, Virginia: Williamsburg, Virginia, College of William and Mary, B. S. thesis in geology, 80 p.